

Dynamics of cosmological perturbations in modified Brans-Dicke cosmology with matter-scalar field interaction

Georgios Kofinas^{1,*} and Nelson A. Lima^{2,†}¹*Research Group of Geometry, Dynamical Systems and Cosmology, Department of Information and Communication Systems Engineering University of the Aegean, Karlovassi 83200, Samos, Greece*²*Institut für Theoretische Physik, Ruprecht-Karls-Universität Heidelberg,**Philosophenweg 16, 69120 Heidelberg, Germany*

(Received 27 April 2017; published 5 October 2017)

In this work we focus on a novel completion of the well-known Brans-Dicke theory that introduces an interaction between the dark energy and dark matter sectors, known as complete Brans-Dicke (CBD) theory. We obtain viable cosmological accelerating solutions that fit supernovae observations with great precision without any scalar potential $V(\phi)$. We use these solutions to explore the impact of the CBD theory on the large scale structure by studying the dynamics of its linear perturbations. We observe a growing behavior of the lensing potential Φ_+ at late-times, while the growth rate is actually suppressed relatively to Λ CDM, which allows the CBD theory to provide a competitive fit to current RSD measurements of $f\sigma_8$. However, we also observe that the theory exhibits a pathological change of sign in the effective gravitational constant concerning the perturbations on subhorizon scales that could pose a challenge to its validity.

DOI: [10.1103/PhysRevD.96.084016](https://doi.org/10.1103/PhysRevD.96.084016)

I. INTRODUCTION

Two decades after the discovery of the late-times accelerated expansion of our Universe [1,2], comprehending the physical nature behind the effect stands as one of the more important challenges in modern physics. In the standard model of cosmology, the Λ cold dark matter (Λ CDM) model, a negative-pressure cosmological constant Λ makes the majority of the energy density in the present cosmos and accelerates its expansion within the framework of Einstein's general relativity (GR). In the concordance model, Λ is attributed to a vacuum energy, but its observed value is inexplicably small to theory (for a review on Λ see [3]).

Hence, modified theories of gravity (MGT) were introduced to explain our Universe's accelerated expansion as an alternative to Λ CDM. Scalar-tensor gravity theories are widely studied as alternatives to general relativity and can play a significant role in the description of the early or late-times cosmic evolution. However, presently, it is not clear that scalar-tensor theories, such as Brans-Dicke (BD) [4], Galileon theory [5], $f(R)$ models [6], and many others embedded within the Horndeski formalism [7] can provide self-accelerating solutions compatible with cosmological observations [8], and hence be genuine alternatives to Λ or dark energy (DE) (for a review on MGT and DE see [9–11]).

In BD gravity in particular, the scalar field forms the dark energy or can play a role in the early Universe

history, but also controls the evolution of the gravitational constant. However, it is well known that in standard BD theory self-accelerating solutions are not compatible with Solar-System constraints [12,13] or even the latest cosmic microwave background (CMB) results [14,15], as these require a negative, order-unity Brans-Dicke parameter ω_{BD} [16,17]. In order to avoid this issue one either adds a self-interacting potential [18–20] or considers a field or time-dependent ω_{BD} [21], but even then the problem is not completely solved. Additionally, nonminimal couplings to matter have been considered in Refs. [22–25].

Most of the cosmological models consider that the evolution of dark matter and dark energy occur separately. This means that the matter Lagrangian is added minimally to the action. In Ref. [26] it was argued that there are observational evidences which indicate a dark matter-dark energy interaction and violation of the equivalence principle between baryons and dark matter. There is a rising activity in cosmology in the study of such interacting models (e.g. [27,28]) which can also help to the solution of the coincidence problem [29,30]. Usually, such interactions are chosen arbitrarily and do not arise by any physical theory. In the context of BD gravity an energy exchange model with a modified wave equation for the scalar field was considered in Ref. [31] (for other approaches with modified equations of motion see [32–35]).

In this work, we focus on a novel extension of the BD theory introduced in Ref. [36], where the simple wave equation of the scalar field was preserved, while the standard conservation of matter was relaxed. Analyzing exhaustively the Bianchi identities, three completions of Brans-Dicke gravity were found to be the only theories

*gkofinas@aegean.gr

†n.lima@thphys.uni-heidelberg.de

which are unambiguously determined from consistency. Here, we will focus on the first of these theories that we will call for brevity as complete Brans-Dicke theory (CBD). This theory has an extra parameter ν that naturally appears as an integration constant, which controls the energy exchange between the dark energy and matter sectors, and when set to zero allows one to recover the standard Brans-Dicke field equations. Although BD gravity was initially formulated in terms of an action solely based on dimensional arguments with the matter Lagrangian being minimally coupled, CBD theory was derived at the level of the equations of motion. The reason is that in the presence of interactions between the matter Lagrangian and the scalar field, there is an infinite number of actions that can be constructed which recover the standard BD action in the absence of interactions.

A discussion on the action of CBD theory was given in Ref. [37], where it was shown that, for a matter Lagrangian that vanishes on shell (such as pressureless dust, for example), the theory can not be recast as a minimally coupled scalar-tensor theory in either the Einstein or Jordan frame. Hence, it should be able to produce interesting phenomenology that cannot be associated to standard Brans-Dicke gravity. Furthermore, and more importantly, the complete BD theory is capable of providing self-accelerating solutions for negative values of this new constant in the absence of a scalar field potential [38]. However, these solutions have not yet been fully explored.

Therefore, in this work, we set out to study the impact these solutions can have on the large scale structure of the Universe by analyzing the dynamics of their linear perturbations. Presently, there is an effort to obtain constraints on modified theories of gravity on larger scales that are competitive with those we have on Solar-System scales, with a surge of surveys in the next decade that will improve our knowledge of the Universe on cosmological scales, such as the Dark Energy Survey (DES) [39], the extended Baryon Oscillation Spectroscopic Survey (eBOSS) [40] and the Euclid survey [41] (for a review on cosmological tests of gravity see [42]). Hence, it is of paramount importance to understand how a particular theory modifies the observable Universe.

This paper is organized as follows: in Sec. II we introduce the complete Brans-Dicke theory and its field equations, and also extend its background solutions presented in Ref. [38] to high redshifts. Then, in Sec. III we derive the full set of perturbed equations of motion and present them in the Newtonian and synchronous gauges. In Sec. IV we present the dynamical first-order differential equations for the lensing potential, Φ_+ , and the slip between the Newtonian potentials, χ , that we numerically evolve to study the dynamics of the linear perturbations. We then derive the subhorizon approximation for the Newtonian potentials in Sec. V, and compute the evolution of the growth rate $f\sigma_8$ in Sec. VI, concluding in Sec. VII.

II. COSMOLOGY IN THE COMPLETE BRANS-DICKE THEORY

We consider the complete Brans-Dicke theory presented in [36] and described by the following equations

$$G^\mu{}_\nu = \frac{8\pi}{\phi} (T^\mu{}_\nu + \mathcal{T}^\mu{}_\nu) \quad (2.1)$$

$$\begin{aligned} T^\mu{}_\nu = & \frac{\phi}{2\lambda(\nu + 8\pi\phi^2)^2} \{2[(1 + \lambda)\nu + 4\pi(2 - 3\lambda)\phi^2]\phi^{;\mu}\phi_{;\nu} \\ & - [(1 + 2\lambda)\nu + 4\pi(2 - 3\lambda)\phi^2]\delta^\mu{}_\nu\phi^{;\rho}\phi_{;\rho}\} \\ & + \frac{\phi^2}{\nu + 8\pi\phi^2} (\phi^{;\mu}{}_{;\nu} - \delta^\mu{}_\nu\Box\phi) \end{aligned} \quad (2.2)$$

$$\Box\phi = 4\pi\lambda\mathcal{T} \quad (2.3)$$

$$T^\mu{}_{\nu;\mu} = \frac{\nu}{\phi(\nu + 8\pi\phi^2)} T^\mu{}_\nu\phi_{;\mu}. \quad (2.4)$$

Compared to the standard Brans-Dicke theory, the new characteristic of these equations is the appearance of the parameter ν , with dimensions mass to the fourth, which enters the gravitational field equations. And, at the same time, it violates the exact conservation of the matter energy-momentum tensor $T^\mu{}_\nu$ in Eq. (2.4). The parameter $\lambda \neq 0$ is related to the standard Brans-Dicke parameter $\omega_{BD} = \frac{2-3\lambda}{2\lambda}$. The system (2.1)–(2.4) reduces for $\nu = 0$ to the Brans-Dicke equations of motion (in units where the velocity of light is set to unit)

$$G^\mu{}_\nu = \frac{8\pi}{\phi} (T^\mu{}_\nu + \mathcal{T}^\mu{}_\nu) \quad (2.5)$$

$$T^\mu{}_\nu = \frac{2 - 3\lambda}{16\pi\lambda\phi} \left(\phi^{;\mu}\phi_{;\nu} - \frac{1}{2}\delta^\mu{}_\nu\phi^{;\rho}\phi_{;\rho} \right) + \frac{1}{8\pi} (\phi^{;\mu}{}_{;\nu} - \delta^\mu{}_\nu\Box\phi) \quad (2.6)$$

$$\Box\phi = 4\pi\lambda\mathcal{T} \quad (2.7)$$

$$T^\mu{}_{\nu;\mu} = 0, \quad (2.8)$$

which is described by the action

$$\begin{aligned} S_{BD} = & \frac{1}{16\pi} \int d^4x \sqrt{-g} \left(\phi R - \frac{\omega_{BD}}{\phi} g^{\mu\nu} \phi_{;\mu}\phi_{;\nu} \right) \\ & + \int d^4x \sqrt{-g} L_m, \end{aligned} \quad (2.9)$$

where $L_m(g_{\kappa\lambda}, \Psi)$ is the matter Lagrangian depending on some extra fields Ψ . The system of equations (2.1) and (2.4) will be analyzed for both a cosmological background and for its perturbations.

For the theory (2.1)–(2.4), a statistically spatially homogeneous and isotropic universe with Friedmann-Robertson-Walker (FRW) metric has been studied in [38]. Here, we consider the spatially flat case with background metric

$$d\bar{s}^2 = -a^2 d\tau^2 + a^2(\tau)\delta_{ij}dx^i dx^j, \quad (2.10)$$

where τ is the conformal time and we will denote with an overdot the derivative with respect to τ . The modified Friedmann equations, the dynamical Brans-Dicke scalar field equation and the energy-momentum conservation equation are given by

$$\mathcal{H}^2 = \frac{8\pi}{3\varphi}\rho a^2 - \frac{8\pi\varphi}{\nu + 8\pi\varphi^2}\mathcal{H}\dot{\varphi} + \frac{4\pi\nu + 4\pi(2-3\lambda)\varphi^2}{3\lambda(\nu + 8\pi\varphi^2)^2}\dot{\varphi}^2 \quad (2.11)$$

$$2\dot{\mathcal{H}} + \mathcal{H}^2 = -\frac{8\pi}{\varphi}\left[pa^2 + \frac{\varphi(1+2\lambda)\nu + 4\pi(2-3\lambda)\varphi^2}{(\nu + 8\pi\varphi^2)^2}\dot{\varphi}^2 + \frac{\varphi^2}{\nu + 8\pi\varphi^2}(\mathcal{H}\dot{\varphi} + \ddot{\varphi})\right] \quad (2.12)$$

$$\ddot{\varphi} + 2\mathcal{H}\dot{\varphi} + 4\pi\lambda(3p - \rho)a^2 = 0 \quad (2.13)$$

$$\dot{\rho} + 3\mathcal{H}(\rho + p) = \frac{\nu}{\varphi(\nu + 8\pi\varphi^2)}\rho\dot{\varphi}, \quad (2.14)$$

with $\mathcal{H} \equiv \frac{\dot{a}}{a} = aH$ the conformal Hubble factor, where $H = \frac{1}{a}\frac{da}{dt}$ is the Hubble parameter ($dt = a d\tau$). The background scalar field is denoted by $\varphi(\tau)$, while in the next section where perturbations will be introduced, the total perturbed field will be $\phi = \varphi + \delta\phi$, with $\delta\phi$ representing the perturbation. Equation (2.14) can be integrated into a simple expression for the evolution of the matter energy density as a function of time

$$\rho = \frac{\rho_*}{a^{3(1+w)}} \frac{\varphi}{\sqrt{|\nu + 8\pi\varphi^2|}}, \quad (2.15)$$

where $\rho_* > 0$ is an integration constant and it is assumed that $\varphi > 0$.

We can write the Friedmann equations (2.11) and (2.12) in a more familiar form

$$\mathcal{H}^2 = \frac{8\pi a^2}{3\varphi}(\rho + \rho_{\text{DE}}) \quad (2.16)$$

$$2\dot{\mathcal{H}} + \mathcal{H}^2 = -\frac{8\pi a^2}{\varphi}(p + p_{\text{DE}}), \quad (2.17)$$

where we have defined the effective dark energy and effective dark pressure as

$$\rho_{\text{DE}} a^2 \equiv -\frac{3\varphi^2}{\nu + 8\pi\varphi^2}\mathcal{H}\dot{\varphi} + \frac{\varphi\nu + 4\pi(2-3\lambda)\varphi^2}{2\lambda(\nu + 8\pi\varphi^2)^2}\dot{\varphi}^2 \quad (2.18)$$

$$p_{\text{DE}} a^2 \equiv \frac{\varphi(1+2\lambda)\nu + 4\pi(2-3\lambda)\varphi^2}{2\lambda(\nu + 8\pi\varphi^2)^2}\dot{\varphi}^2 + \frac{\varphi^2}{\nu + 8\pi\varphi^2}(\mathcal{H}\dot{\varphi} + \ddot{\varphi}). \quad (2.19)$$

Then, according to (2.16), the density parameters are defined as

$$\Omega_{\text{m}} = \frac{8\pi\rho a^2}{3\varphi\mathcal{H}^2}, \quad \Omega_{\text{DE}} = \frac{8\pi\rho_{\text{DE}} a^2}{3\varphi\mathcal{H}^2}. \quad (2.20)$$

In Ref. [38], the numerical background solutions were obtained integrating the Friedmann and the scalar field equations backwards in time, from a present-day value of the scale factor normalized to 1, i.e. $a_0 = 1$. Hence, the value of the integration constant ρ_* was set so that Ω_{m} today, Ω_{m}^0 , would be equal to a fixed value close to 0.30. Then, the units were chosen so that the initial value of the scalar field, φ_0 , was fixed to be 1. The present-day value of the scalar field velocity $\dot{\varphi}_0$ and the parameters λ, ν were constrained so that Ω_{DE}^0 has the value $1 - \Omega_{\text{m}}^0$ and also that the value of the effective dark energy equation of state $w_{\text{DE}} = p_{\text{DE}}/\rho_{\text{DE}}$ was close to -1 today, with matter domination at earlier times. Using this “backward” method, the solutions obtained provided self-acceleration at the present for different values of ν and λ . However, the stability of the solutions obtained with this method toward very high redshifts is not guaranteed, which we have numerically checked.

In this work, we are interested in obtaining the evolution of linear perturbations from deep within matter domination. We attempt to perform a forward numerical evolution from a high redshift $z_i \gg 1$, so the initial conditions are set at $z_i = 1000$. We choose to use the logarithmic variable $N = \ln a$ as the integration variable, thus its initial value is $N_i = -6.91$ (while today we still have $a_0 = 1$). The system of equations (2.11), (2.12), and (2.13), after using Eq. (2.15), is written equivalently as

$$\frac{4\pi\nu + 4\pi(2-3\lambda)\varphi^2}{3\lambda(\nu + 8\pi\varphi^2)^2}\varphi'^2 - \frac{8\pi\varphi}{\nu + 8\pi\varphi^2}\varphi' + \frac{8\pi\rho_* e^{-N}}{3\mathcal{H}^2\sqrt{|\nu + 8\pi\varphi^2|}} - 1 = 0 \quad (2.21)$$

$$\frac{2}{\mathcal{H}}\mathcal{H}' + \frac{4\pi(1+2\lambda)\nu + 4\pi(2-3\lambda)\varphi^2}{\lambda(\nu + 8\pi\varphi^2)^2}\varphi'^2 + \frac{8\pi\varphi}{\nu + 8\pi\varphi^2}\left(\frac{4\pi\lambda\rho_*\varphi e^{-N}}{\mathcal{H}^2\sqrt{|\nu + 8\pi\varphi^2|}} - \varphi'\right) + 1 = 0 \quad (2.22)$$

$$\varphi'' + \left(2 + \frac{\mathcal{H}'}{\mathcal{H}}\right)\varphi' - \frac{4\pi\lambda\rho_*\varphi e^{-N}}{\mathcal{H}^2\sqrt{|\nu + 8\pi\varphi^2|}} = 0, \quad (2.23)$$

where a prime denotes a derivative with respect to N . The system (2.21)–(2.23) contains the integration constant ρ_* and the parameters λ , ν that have to be specified. It is a consistent system since equation (2.21) is the constraint. The analysis of this system can be made in two ways. In the first one, the quantity $e^{-N}\mathcal{H}^{-2}$ is replaced from (2.21) into (2.22) and (2.23), and then, an autonomous second-order differential equation for φ arises. When this equation is solved for $\varphi(N)$, then $\mathcal{H}(N)$ is found algebraically from (2.21). In this method we need at the initial time N_i the two initial conditions φ_i , φ'_i . In the second way, Eqs. (2.21) and (2.22) are viewed as a system of two first-order differential equations for φ , \mathcal{H} . Now, we need at the initial time N_i the two initial values φ_i , \mathcal{H}_i [of course, φ'_i can be found from (2.21)].

From the physical point of view the evolution should be such that at early times the contribution of the effective dark energy density is negligible, i.e. $\Omega_{\text{DE}} \ll 1$. As seen from (2.18), the simplest condition in order for this to be achieved is to choose $|\varphi'_i| \ll 1$, and the standard GR behaviour is recovered at early times. This implies from equation (2.21) the value of ρ_* in terms of the initial values φ_i , H_i , i.e. $\rho_* = (3/8\pi)a_i^3 H_i^2 \sqrt{|\nu + 8\pi\varphi_i^2|}$. Therefore, there are not three independent integration constants, but only two. In Λ CDM there are two integration constants, namely H_i , ρ_* , while the condition of negligible initial dark energy is automatically satisfied, since at z_i the matter term is 10^9 times larger than the cosmological constant term, therefore the two initial data are set at present in agreement with the values H_0 , Ω_m^0 .

Then, we fix the free parameters λ and ν . From (2.18) we need to set λ such that $\lambda \gtrsim |\varphi'_i|$ in order to keep $\Omega_{\text{DE}} \ll 1$. In this work, we choose $\lambda = 1$. In Ref. [38], it was shown that the condition $\nu + 8\pi\varphi^2 < 0$ is successful in order to have accelerating solutions today. Although acceleration also appeared in some cases where the above quantity is positive, here we will assume the negative sign and set ν to a high negative value of -100 . Therefore, a solution should be restricted to the branch with $\varphi < \varphi_\infty = \sqrt{|\nu|/(8\pi)}$, otherwise poles would appear in the equations, e.g. in Eq. (2.15) for the energy density. One word about the units is needed at this point. Since φ^{-1} plays the role of varying gravitational constant G , the scalar field φ has dimensions of mass squared. Therefore, dimensionless quantities $\hat{\varphi}$, $\hat{\nu}$ can be defined as $\hat{\varphi} = G_N \varphi$ and $\hat{\nu} = G_N^2 \nu$, where G_N is Newton's constant. Then, in all the previous equations we should replace φ by $\hat{\varphi}$, ν by $\hat{\nu}$, and all ρ_* , ρ , p , ρ_{DE} , p_{DE} should be multiplied by G_N . In this sense, in the numerical analysis, when we say that ν is -100 , we strictly mean that $\hat{\nu}$ is -100 , while an order one value of φ basically means of $\hat{\varphi}$. Moreover, it should be noted that the parameter ν can be

totally absorbed in the system (2.21)–(2.23) when the rescaling $\varphi \rightarrow \varphi/\sqrt{|\nu|}$, $\rho_* \rightarrow \rho_*/\sqrt{|\nu|}$ is performed.

Since $|\varphi'_i| \ll 1$, in the first period of evolution it is $\varphi \approx \varphi_i$, thus in equation (2.11) the derivatives of φ can be omitted and we obtain $H^2 \approx a_i^3 H_i^2 a^{-3}$, which is the behaviour of Einstein gravity in matter era. Instead of having the unknown dimensionful initial value H_i in the above expression of H^2 , as well as in ρ_* , we prefer to normalize H_i to the central value $\hat{H}_0 = 67.8$ km/s/Mpc coming from the latest Planck data, and parametrize H_i in terms of the dimensionless quantity $\hat{\Omega}_m$ as follows: $a_i^3 H_i^2 = \hat{H}_0^2 \hat{\Omega}_m$. Therefore, it is $H^2 \approx \hat{H}_0^2 \hat{\Omega}_m a^{-3}$ initially, and $\rho_* = (3/8\pi)\hat{H}_0^2 \hat{\Omega}_m \sqrt{|\nu + 8\pi\varphi_i^2|}$. The quantity $\hat{\Omega}_m$ can be interpreted as a fictitious value of the density parameter Ω_m corresponding to the energy density ρ_* .

It is obvious that since the initial data are set at an early epoch, the evolution of the equations does not assure that the evolved theoretical today values $H(a=1)$, $\Omega_m(a=1)$ will coincide with the actual today values H_0 , Ω_m^0 . Of course, the values H_0 , Ω_m^0 are known from observations not precisely, but with a small uncertainty. The value of Ω_m^0 is close to 0.30 according to the most recent constraints [43]. Therefore, $H(a=1)$, $\Omega_m(a=1)$ should be close to the values \hat{H}_0 , 0.3 respectively, still within local observable bounds. As a result, the two integration constants $\hat{\Omega}_m$, φ_i , which determine the whole evolution, cannot be chosen arbitrarily, but should provide consistent values of $H(a=1)$, $\Omega_m(a=1)$. In the following we will succeed in such an agreement between these theoretical and observed values by fixing appropriately the initial conditions. Actually, we will be more precise than that and provide a very good fit to low-redshift supernovae data. As for the density parameter, it arises that at all times it is $\Omega_m = \hat{H}_0^2 \hat{\Omega}_m \sqrt{|\nu + 8\pi\varphi_i^2|} / (e^{3N} H^2 \sqrt{|\nu + 8\pi\varphi^2|})$. Initially, $\Omega_m^i = 1$, thus the condition for ρ_* is found as above. Today,

$$\Omega_m(a=1) = \hat{\Omega}_m \sqrt{\frac{|\nu + 8\pi\varphi_i^2|}{|\nu + 8\pi\varphi_0^2|}} \frac{\hat{H}_0^2}{H^2(a=1)}, \quad (2.24)$$

where we denote by φ_0 the value of $\varphi(a=1)$ resulting from the numerical evolution, since there is no observational constraint on the present value of the scalar field to distinguish between φ_0 and $\varphi(a=1)$. Although φ^{-1} is interpreted as the varying gravitational constant G , this does not mean that φ_0 equals G_N^{-1} . It is actually expected that φ_0 is of the order of G_N^{-1} , but the precise numerical value is an issue of the initial conditions appropriate to explain the current state of the Universe determined by H_0 , Ω_m^0 . According to (2.24), successful $\hat{\Omega}_m$, φ_i should provide that $H(a=1)$ is approximately equal to \hat{H}_0 , and also that φ_0 agrees with the value provided by (2.24) with $\Omega_m(a=1)$ close to 0.3. Thus, it is not an easy task to find such $\hat{\Omega}_m$, φ_i .

Since we have assumed that $\nu + 8\pi\varphi^2 < 0$, it will be verified numerically that the scalar field grows in time (it is

actually expected that G decreases with time), thus $\varphi_0 > \varphi_i$. Since $H(a=1)$, $\Omega_m(a=1)$ must be close to \hat{H}_0 , 0.3, it arises from (2.24) that $\hat{\Omega}_m < 0.3$. This will implicate a larger separation between the cosmological evolutions predicted by the complete Brans-Dicke theory and Λ CDM at early-times than at late-times. We have implemented a Brent algorithm that searches for the right φ_i in order to yield the desired $\Omega_m(a=1)$ for a chosen $\hat{\Omega}_m$. The latter was fine-tuned to produce a value of $H(a=1)$ that is compatible with current observations. In the figures shown in this section we have used $\hat{\Omega}_m = 0.17$ and $\varphi_i = 0.029$, thus $\varphi_0 = 1.773$ and $H_i = \hat{H}_0 \sqrt{\hat{\Omega}_m} (1+z_i)^{3/2} = 13058 \hat{H}_0$. The function $a(\tau)$ can be found numerically from the numerical solution $\mathcal{H}(N)$.

Another equivalent system of differential equations can be presented which eliminates the initial condition $\hat{\Omega}_m$ and at the same time it only needs to conform with a consistent value of $\Omega_m(a=1)$, thus it facilitates the search for appropriate initial conditions. A rewriting of Eqs. (2.21) and (2.22) gives a system for the evolution of φ and Ω_m as

$$\frac{4\pi\nu + 4\pi(2-3\lambda)\varphi^2}{3\lambda(\nu + 8\pi\varphi^2)^2} \varphi'^2 - \frac{8\pi\varphi}{\nu + 8\pi\varphi^2} \varphi' + \Omega_m - 1 = 0 \quad (2.25)$$

$$\begin{aligned} \frac{\Omega'_m}{\Omega_m} - \frac{4\pi(1+2\lambda)\nu + 4\pi(2-3\lambda)\varphi^2}{\lambda(\nu + 8\pi\varphi^2)^2} \varphi'^2 \\ - \frac{4\pi\varphi}{\nu + 8\pi\varphi^2} (3\lambda\varphi\Omega_m - 4\varphi') = 0. \end{aligned} \quad (2.26)$$

Initially it is $\Omega_m^i = 1$ and only the initial condition φ_i is free. Moreover, this system does not need to match the

value $H(a=1)$, but only that of $\Omega_m(a=1)$. Therefore, scanning the parameter φ_i to provide $\Omega_m(a=1) = 0.30$ is relatively easier, and the same values of φ_i , φ_0 are found as above. From the numerical solutions $\varphi(N)$, $\Omega_m(N)$, a suitable $\hat{\Omega}_m$ is selected as before that provides algebraically the function $H(N)$ which possesses sufficient fitting to the supernovae.

In Fig. 1 we plot the background evolution predicted by CBD according to the explanations of the previous paragraphs. In Fig. 1(a) we have the Hubble parameter as a function of the scale factor, compared against the evolution predicted by the standard model, Λ CDM. As expected, we have a larger separation between both cosmologies at earlier times. Today, we have a less than 10% difference between both models, with the present-day value of H predicted by the CBD equal to $H(a=1) = 73.4$ km/s/Mpc, compatible with local measurements of the Hubble parameter [44–46].

Then, in Fig. 1(b) we plot $\Omega_m(a)$ and $\Omega_{DE}(a)$. We see that our model provides a stable matter dominated phase that is gradually overtaken by the effective dark energy component close to the present, yielding $\Omega_m^0 = 0.30$ and $\Omega_{DE}^0 = 0.7$. We also note that the flatness of the Universe is guaranteed as we have numerically checked to have $\Omega_m + \Omega_{DE} = 1$ throughout the cosmological evolution. The viability of our model is further corroborated by the evolution of the deceleration parameter $q = -1 - \frac{1}{H^2} \frac{dH}{dt} = -\frac{\ddot{H}}{H^2}$ in Fig. 1(b), where we clearly observe the transition from a decelerating to an accelerating dark energy dominated Universe close to the present-day. We have also checked that the model asymptotically tends to the value φ_∞ without crossing it, therefore avoiding any singularity on the Hubble parameter and its derivatives. As φ approaches φ_∞ , the first term on the right hand side of

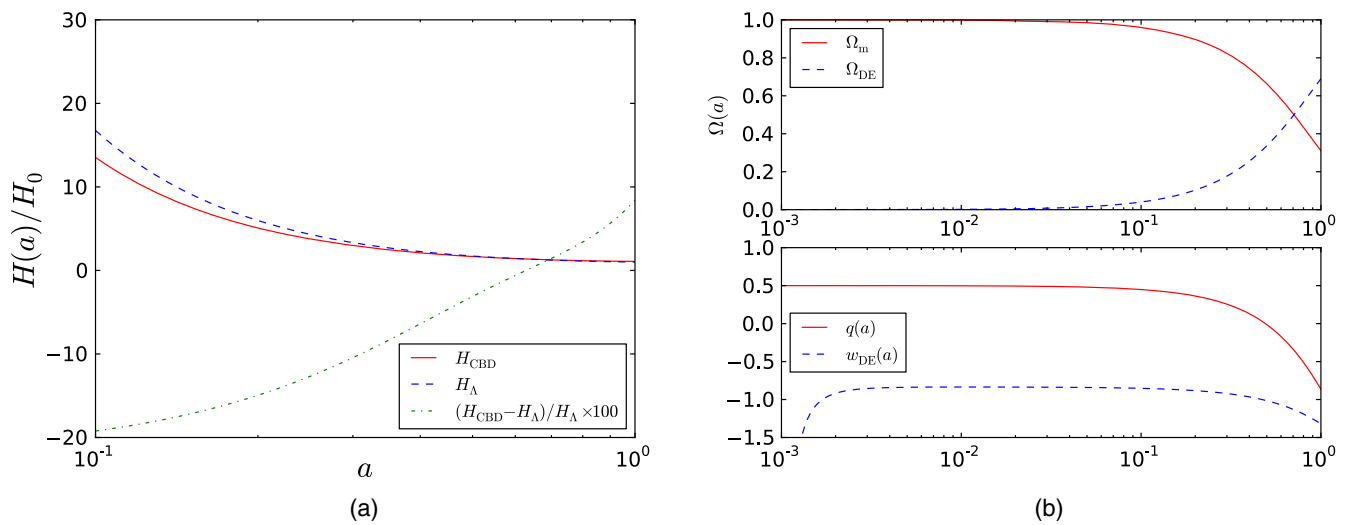


FIG. 1. We plot the background evolution predicted by the complete Brans-Dicke for the following choice of parameters: $\lambda = 1$, $\nu = -100$, $\hat{\Omega}_m = 0.17$ and $\varphi_i = 0.029$. In (a) we have the evolution of the Hubble parameter against Λ CDM; in (b) we plot the evolution of Ω_m and Ω_{DE} , together with the deceleration parameter q and the effective dark energy equation of state w_{DE} .

Eq. (2.18), which is positive, becomes enhanced and dominates the negative second term, ensuring a positive Ω_{DE} .

Still in Fig. 1(b), we also have the evolution of the effective dark energy equation of state, w_{DE} , where we see that our solution predicts a phantom behavior today by having $w_{\text{DE},0} < -1$. For completeness, we also comment on the early-time behavior of w_{DE} , where we note that the effective equation of state tends toward increasingly larger negative values. This is a consequence of the way we have set our initial conditions. Equation (2.18) shows that ρ_{DE} will tend toward negligibly smaller values at early-times the closer we set ϕ'_i to zero, leading to larger negative values in w_{DE} . This has, however, no discernible impact in the background evolution, we predict, as Ω_{DE} is also negligible at the epoch we set the initial conditions.

Lastly, in Fig. 2, we compare our model to data from the Union 2.1 compilation of 580 Type Ia supernova [47], from which we adopt the covariance matrix without the presence of systematics. We see that our model fits the data with remarkable precision, comparable to ΛCDM , without the presence of a potential. Hence, having a complete Brans-Dicke model that predicts a viable background history and fits existing data, we can proceed to obtain the evolution of the linear perturbations in this theory.

III. PERTURBATION THEORY

We will study the scalar perturbations of the theory (2.1)–(2.4) around the background (2.10). So, the background spatial metric is taken to be flat across all scales comparable to the wavelength of the perturbations. The spatial harmonic functions satisfying the equation

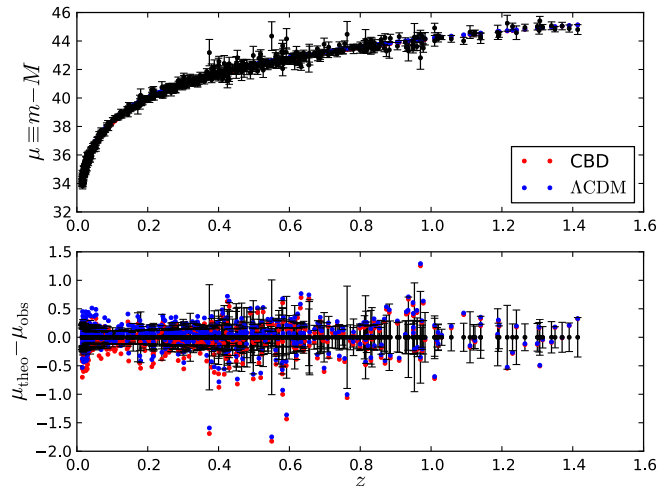


FIG. 2. We plot the distance moduli $\mu \equiv m - M$ predicted by our model (using the parameters of Fig. 1) and ΛCDM , and compare to the Union 2.1 compilation from the Supernova Cosmology Project [47]. For the error bars, we adopted the covariance matrix without systematics.

$(\nabla^2 + k^2)Y = 0$ are a complete set of the simple plane waves

$$Y(\vec{k}, \vec{x}) \propto e^{i\vec{k}\cdot\vec{x}}, \quad (3.1)$$

where $\nabla^2 = \delta^{ij}\partial_i\partial_j$, $k^2 = \delta_{ij}k^ik^j$, and $\vec{k}\cdot\vec{x} = \delta_{ij}k^ix^j$. In order to expand perturbations, scalars are expanded by Y , while vectors and tensors are expanded respectively by

$$Y_i = -\frac{1}{k}Y_{,i} = -i\frac{k_i}{k}Y \quad (3.2)$$

$$Y_{ij} = \frac{1}{k^2}Y_{,ij} + \frac{1}{3}\delta_{ij}Y = \left(\frac{1}{3}\delta_{ij} - \frac{k_ik_j}{k^2}\right)Y. \quad (3.3)$$

For a scalar perturbation the perturbed metric tensor $g_{\mu\nu}$ for a given wave-number k is generally parametrized in terms of four independent functions of time A , B , H_L , H_T as [48]

$$ds^2 = g_{00}d\tau^2 + 2g_{0i}d\tau dx^i + g_{ij}dx^i dx^j, \quad (3.4)$$

where

$$g_{00} = -a^2(1 + 2AY) \quad (3.5)$$

$$g_{0i} = -a^2BY_i \quad (3.6)$$

$$g_{ij} = a^2(\delta_{ij} + 2H_L Y\delta_{ij} + 2H_T Y_{ij}). \quad (3.7)$$

The perturbed scalar field is written as $\phi = \varphi(\tau) + \chi(\tau)Y$, where φ is the background field and χ the time dependent part of the perturbation. The formulas for the perturbations of various geometric quantities as well as of the scalar field derivatives are given in the Appendix.

The perturbations in the stress-energy tensor are decomposed into four components: density $\delta\rho = \rho\delta = \rho\delta Y$ [with $\rho(\tau)$ the background density and $\delta(\tau)$ the amplitude of density perturbation], velocity v (where the perturbed spatial velocity is $\frac{u^i}{u^0} = vY^i$), isotropic pressure $\delta p = \varpi Y$ [with $\varpi(\tau)$ measuring the amplitude of isotropic pressure perturbation], and anisotropic stress $\frac{3}{2}(\rho + p)\sigma(\tau)$ in agreement with [49]. The perturbed stress-energy tensor takes the form

$$\begin{aligned} T^0_0 &= -\rho(1 + \delta Y), \\ T^0_i &= (\rho + p)(v - B)Y_i, \\ T^i_j &= (p + \varpi Y)\delta^i_j + \frac{3}{2}(\rho + p)\sigma Y^i_j. \end{aligned} \quad (3.8)$$

The linearized version of the nonconservation law (2.4) is expressed as dynamical equations for the energy density contrast δ and the velocity v as follows

$$\begin{aligned} \dot{\delta} + (1+w)(kv + 3\dot{H}_L) + 3\mathcal{H}\left(\frac{\delta p}{\delta\rho} - w\right)\delta \\ = \frac{\nu}{\varphi(\nu + 8\pi\varphi^2)}\dot{\chi} - \frac{\nu(\nu + 24\pi\varphi^2)}{\varphi^2(\nu + 8\pi\varphi^2)^2}\dot{\varphi}\chi \end{aligned} \quad (3.9)$$

$$\begin{aligned} \dot{v} - \dot{B} + (1-3w)\mathcal{H}(v-B) + \frac{\dot{w}}{1+w}(v-B) - \frac{\delta p/\delta\rho}{1+w}k\delta \\ - kA + k\sigma = -\frac{\nu}{\varphi(\nu + 8\pi\varphi^2)}\frac{w}{1+w}k\chi, \end{aligned} \quad (3.10)$$

where $w = p/\rho$ is the barotropic index of the background single fluid and $\frac{\delta p}{\delta\rho}\delta = \frac{\varpi}{\rho}$. Note that the nonconservation Eq. (2.4) for the background has been used in the derivation of (3.9) and (3.10). We will consider that the evolution starts deep within matter domination and neglects radiation. Hence, \dot{w} will be set to zero and we will have just the matter component.

Next we proceed with the four perturbed field equations (2.1) which give

0-0 component

$$\begin{aligned} \varphi \left[3\mathcal{H}^2 A - k\mathcal{H}B - 3\mathcal{H}\dot{H}_L - k^2 \left(H_L + \frac{H_T}{3} \right) \right] \\ - \frac{3}{2}\mathcal{H}^2\chi = 4\pi(-\rho a^2\delta + \tau_1) \end{aligned} \quad (3.11)$$

$$\begin{aligned} \tau_1 = \frac{24\pi\varphi^2 - \nu}{2\lambda(\nu + 8\pi\varphi^2)^3} [\nu + 4\pi(2-3\lambda)\varphi^2]\dot{\varphi}^2\chi \\ + \frac{\varphi\dot{\varphi}}{\lambda(\nu + 8\pi\varphi^2)^2} \{ [\nu + 4\pi(2-3\lambda)\varphi^2](\dot{\varphi}A - \dot{\chi}) \\ - 4\pi(2-3\lambda)\varphi\dot{\varphi}\chi \} + \frac{6\nu\varphi\dot{\varphi}}{(\nu + 8\pi\varphi^2)^2}\mathcal{H}\chi \\ + \frac{\varphi^2}{\nu + 8\pi\varphi^2} [k^2\chi + 3\mathcal{H}\dot{\chi} - \dot{\varphi}(6\mathcal{H}A - kB - 3\dot{H}_L)], \end{aligned} \quad (3.12)$$

0-i component

$$\begin{aligned} \varphi \left(\mathcal{H}A - \dot{H}_L - \frac{1}{3}\dot{H}_T \right) \\ = \frac{4\pi\varphi^2}{\nu + 8\pi\varphi^2} (\dot{\chi} - \mathcal{H}\chi - \dot{\varphi}A) \\ + \frac{4\pi\varphi}{\lambda(\nu + 8\pi\varphi^2)^2} [\nu(1+\lambda) + 4\pi(2-3\lambda)\varphi^2]\dot{\varphi}\chi \\ + \frac{4\pi}{k}(1+w)\rho a^2(v-B), \end{aligned} \quad (3.13)$$

i-j (i ≠ j) component

$$\varphi \left[-k^2 A - k(\dot{B} + \mathcal{H}B) + \ddot{H}_T - k^2 \left(H_L + \frac{H_T}{3} \right) + \mathcal{H}(2\dot{H}_T - kB) \right] = \frac{8\pi\varphi^2}{\nu + 8\pi\varphi^2} [k^2\chi + \dot{\varphi}(kB - \dot{H}_T)] + 12\pi(1+w)\rho a^2\sigma, \quad (3.14)$$

i-i component

$$2\varphi \left[\left(\mathcal{H}^2 + 2\dot{\mathcal{H}} - \frac{k^2}{3} \right) A - \frac{k}{3}(\dot{B} + 2\mathcal{H}B) + \mathcal{H}\dot{A} - \ddot{H}_L - 2\mathcal{H}\dot{H}_L - \frac{k^2}{3} \left(H_L + \frac{H_T}{3} \right) \right] - (\mathcal{H}^2 + 2\dot{\mathcal{H}})\chi = 8\pi(a^2\varpi + \tau_2), \quad (3.15)$$

$$\begin{aligned} \tau_2 = \frac{\nu - 24\pi\varphi^2}{2\lambda(\nu + 8\pi\varphi^2)^3} [(1+2\lambda)\nu + 4\pi(2-3\lambda)\varphi^2]\dot{\varphi}^2\chi + \frac{\varphi^2}{\nu + 8\pi\varphi^2} \left[\frac{2k}{3}\dot{\varphi}B - 2(\ddot{\varphi} + \mathcal{H}\dot{\varphi})A - \dot{\varphi}\dot{A} + \ddot{\chi} + \mathcal{H}\dot{\chi} + \frac{2k^2}{3}\chi + 2\dot{\varphi}\dot{H}_L \right] \\ - \frac{\varphi\dot{\varphi}}{\lambda(\nu + 8\pi\varphi^2)^2} \{ [(1+2\lambda)\nu + 4\pi(2-3\lambda)\varphi^2](\dot{\varphi}A - \dot{\chi}) - 4\pi(2-3\lambda)\varphi\dot{\varphi}\chi \} - \frac{2\nu\varphi}{(\nu + 8\pi\varphi^2)^2} [\mathcal{H}\dot{\varphi} + 4\pi\lambda(3w-1)\rho a^2]\chi. \end{aligned} \quad (3.16)$$

Finally, the perturbed scalar field Eq. (2.3) gives

δφ equation

$$\ddot{\chi} + 2\mathcal{H}\dot{\chi} + k^2\chi - 2\ddot{\varphi}A - \dot{\varphi}(4\mathcal{H}A + \dot{A} - kB - 3\dot{H}_L) = 4\pi\lambda \left(1 - 3\frac{\delta p}{\delta\rho} \right) \rho a^2\delta. \quad (3.17)$$

Because of the Bianchi identities, not all of the above equations are independent, but as for the background, also here, one of these equations plays the role of the constraint. Therefore, one equation is redundant and can be neglected. Since Eq. (3.15) is the most

complicated one containing also second derivatives, we will not make use of this in the numerical analysis of Sec. IV. However, in Sec. V of subhorizon approximation, Eq. (3.15) will be used, while Eq. (3.13) will be the redundant one.

A. Conformal Newtonian gauge

In the Newtonian gauge, one sets $H_T = B = 0$, $A = \Psi$, $H_L = -\Phi$ [49]. The matter equations of motion (3.9), (3.10) take the following form in this gauge

$$\begin{aligned} \dot{\delta} + (1+w)(kv - 3\dot{\Phi}) + 3\mathcal{H}\left(\frac{\delta p}{\delta\rho} - w\right)\delta \\ = \frac{\nu}{\varphi(\nu + 8\pi\varphi^2)}\dot{\chi} - \frac{\nu(\nu + 24\pi\varphi^2)}{\varphi^2(\nu + 8\pi\varphi^2)^2}\dot{\varphi}\chi \end{aligned} \quad (3.18)$$

$$\begin{aligned} \dot{v} + (1-3w)\mathcal{H}v + \frac{\dot{w}}{1+w}v - \frac{\delta p/\delta\rho}{1+w}k\delta - k\Psi + k\sigma \\ = -\frac{\nu}{\varphi(\nu + 8\pi\varphi^2)}\frac{w}{1+w}k\chi. \end{aligned} \quad (3.19)$$

The gravitational equations take the form

0-0 component

$$\varphi(3\mathcal{H}^2\Psi + 3\mathcal{H}\dot{\Phi} + k^2\Phi) - \frac{3}{2}\mathcal{H}^2\chi = 4\pi(-\rho a^2\delta + \tau_1), \quad (3.20)$$

$$\begin{aligned} \tau_1 = \frac{24\pi\varphi^2 - \nu}{2\lambda(\nu + 8\pi\varphi^2)^3}[\nu + 4\pi(2-3\lambda)\varphi^2]\dot{\varphi}^2\chi \\ + \frac{\varphi\dot{\varphi}}{\lambda(\nu + 8\pi\varphi^2)^2} \{[\nu + 4\pi(2-3\lambda)\varphi^2](\dot{\varphi}\Psi - \dot{\chi}) \\ - 4\pi(2-3\lambda)\varphi\dot{\varphi}\chi\} + \frac{6\nu\varphi\dot{\varphi}}{(\nu + 8\pi\varphi^2)^2}\mathcal{H}\chi \\ + \frac{\varphi^2}{\nu + 8\pi\varphi^2}[k^2\chi + 3\mathcal{H}\dot{\chi} - \dot{\varphi}(6\mathcal{H}\Psi + 3\dot{\Phi})], \end{aligned} \quad (3.21)$$

$$\begin{aligned} \tau_2 = \frac{\nu - 24\pi\varphi^2}{2\lambda(\nu + 8\pi\varphi^2)^3}[(1+2\lambda)\nu + 4\pi(2-3\lambda)\varphi^2]\dot{\varphi}^2\chi - \frac{\varphi^2}{\nu + 8\pi\varphi^2} \left[2(\ddot{\varphi} + \mathcal{H}\dot{\varphi})\Psi + \dot{\varphi}\dot{\Psi} + 2\dot{\varphi}\dot{\Phi} - \dot{\chi} - \mathcal{H}\dot{\chi} - \frac{2k^2}{3}\chi \right] \\ - \frac{\varphi\dot{\varphi}}{\lambda(\nu + 8\pi\varphi^2)^2} \{ [(1+2\lambda)\nu + 4\pi(2-3\lambda)\varphi^2](\dot{\varphi}\Psi - \dot{\chi}) - 4\pi(2-3\lambda)\varphi\dot{\varphi}\chi \} - \frac{2\nu\varphi}{(\nu + 8\pi\varphi^2)^2}[\mathcal{H}\dot{\varphi} + 4\pi\lambda(3w-1)\rho a^2]\chi. \end{aligned} \quad (3.25)$$

Finally, the scalar field Eq. (3.17) becomes
 $\delta\phi$ equation

$$\begin{aligned} \ddot{\chi} + 2\mathcal{H}\dot{\chi} + k^2\chi - 2\ddot{\varphi}\Psi - \dot{\varphi}(4\mathcal{H}\Psi + \dot{\Psi} + 3\dot{\Phi}) \\ = 4\pi\lambda\left(1 - 3\frac{\delta p}{\delta\rho}\right)\rho a^2\delta. \end{aligned} \quad (3.26)$$

B. Synchronous gauge

In this gauge, one sets $A = B = 0$, and $H_L = h/6$, $H_T = -3(\eta + h/6)$ [49]. The matter equations of motion (3.9), (3.10) take the following form in this gauge

0-i component

$$\begin{aligned} \varphi(\mathcal{H}\Psi + \dot{\Phi}) \\ = \frac{4\pi\varphi^2}{\nu + 8\pi\varphi^2}(\dot{\chi} - \mathcal{H}\chi - \dot{\varphi}\Psi) + \frac{4\pi\varphi}{\lambda(\nu + 8\pi\varphi^2)^2}[\nu(1+\lambda) \\ + 4\pi(2-3\lambda)\varphi^2]\dot{\varphi}\chi + \frac{4\pi}{k}(1+w)\rho a^2v, \end{aligned} \quad (3.22)$$

i-j (i ≠ j) component

$$\varphi(\Phi - \Psi) = \frac{8\pi\varphi^2}{\nu + 8\pi\varphi^2}\chi + \frac{12\pi}{k^2}(1+w)\rho a^2\sigma, \quad (3.23)$$

i-i component

$$\begin{aligned} 2\varphi \left[\left(\mathcal{H}^2 + 2\dot{\mathcal{H}} - \frac{k^2}{3} \right) \Psi + \frac{k^2}{3} \Phi + \ddot{\Phi} + 2\mathcal{H}\dot{\Phi} + \mathcal{H}\dot{\Psi} \right] \\ - (\mathcal{H}^2 + 2\dot{\mathcal{H}})\chi = 8\pi(a^2\varpi + \tau_2), \end{aligned} \quad (3.24)$$

$$\begin{aligned} \dot{\delta} + (1+w)\left(kv + \frac{\dot{h}}{2}\right) + 3\mathcal{H}\left(\frac{\delta p}{\delta\rho} - w\right)\delta \\ = \frac{\nu}{\varphi(\nu + 8\pi\varphi^2)}\dot{\chi} - \frac{\nu(\nu + 24\pi\varphi^2)}{\varphi^2(\nu + 8\pi\varphi^2)^2}\dot{\varphi}\chi \end{aligned} \quad (3.27)$$

$$\begin{aligned} \dot{v} + (1-3w)\mathcal{H}v + \frac{\dot{w}}{1+w}v - \frac{\delta p/\delta\rho}{1+w}k\delta + k\sigma \\ = -\frac{\nu}{\varphi(\nu + 8\pi\varphi^2)}\frac{w}{1+w}k\chi. \end{aligned} \quad (3.28)$$

One may remove the remaining freedom and completely define the coordinates by setting the cold dark matter

particles are at rest, having zero peculiar velocity v . Indeed, for cold dark matter there is no stress, $\sigma = 0$, and the isotropic pressure perturbation δp should vanish as well since pressure gradients should only be relevant at very small scales (and even then, this is neglected sometimes). Thus, the condition of vanishing peculiar velocity, $v = 0$, is consistent with Eq. (3.28). Of course, such a result is not possible in Newtonian gauge due to the presence of the gravitational potential Ψ in (3.19).

The gravitational equations take the form

0–0 component

$$\varphi(\mathcal{H}\dot{h} - 2k^2\eta) + 3\mathcal{H}^2\chi = 8\pi(\rho a^2\delta - \tau_1), \quad (3.29)$$

$$\begin{aligned} \tau_1 = & \frac{24\pi\varphi^2 - \nu}{2\lambda(\nu + 8\pi\varphi^2)^3} [\nu + 4\pi(2 - 3\lambda)\varphi^2] \dot{\varphi}^2\chi \\ & - \frac{\varphi\dot{\varphi}}{\lambda(\nu + 8\pi\varphi^2)^2} \{[\nu + 4\pi(2 - 3\lambda)\varphi^2]\dot{\chi} + 4\pi(2 - 3\lambda)\varphi\dot{\varphi}\chi\} \\ & + \frac{6\nu\varphi\dot{\varphi}}{(\nu + 8\pi\varphi^2)^2} \mathcal{H}\chi + \frac{\varphi^2}{\nu + 8\pi\varphi^2} \left(k^2\chi + 3\mathcal{H}\dot{\chi} + \frac{\dot{\varphi}}{2}\dot{h} \right), \end{aligned} \quad (3.30)$$

0–i component

$$\begin{aligned} \varphi\dot{\eta} = & \frac{4\pi\varphi^2}{\nu + 8\pi\varphi^2} (\dot{\chi} - \mathcal{H}\chi) + \frac{4\pi\varphi}{\lambda(\nu + 8\pi\varphi^2)^2} [\nu(1 + \lambda) \\ & + 4\pi(2 - 3\lambda)\varphi^2] \dot{\varphi}\chi + \frac{4\pi}{k} (1 + w)\rho a^2 v, \end{aligned} \quad (3.31)$$

i – j (i ≠ j) component

$$\begin{aligned} \varphi \left[k^2\eta - 6\mathcal{H} \left(\dot{\eta} + \frac{\dot{h}}{6} \right) - 3\dot{\eta} - \frac{\ddot{h}}{2} \right] \\ = \frac{8\pi\varphi^2}{\nu + 8\pi\varphi^2} \left[k^2\chi + 3\dot{\varphi} \left(\dot{\eta} + \frac{\dot{h}}{6} \right) \right] + 12\pi(1 + w)\rho a^2 \sigma, \end{aligned} \quad (3.32)$$

i – i component

$$\frac{\varphi}{3} (2k^2\eta - 2\mathcal{H}\dot{h} - \ddot{h}) - (\mathcal{H}^2 + 2\dot{\mathcal{H}})\chi = 8\pi(a^2\varpi + \tau_2), \quad (3.33)$$

$$\begin{aligned} \tau_2 = & \frac{\nu - 24\pi\varphi^2}{2\lambda(\nu + 8\pi\varphi^2)^3} [(1 + 2\lambda)\nu + 4\pi(2 - 3\lambda)\varphi^2] \dot{\varphi}^2\chi + \frac{\varphi^2}{\nu + 8\pi\varphi^2} \left(\dot{\chi} + \mathcal{H}\dot{\chi} + \frac{2k^2}{3}\chi + \frac{\dot{\varphi}}{3}\dot{h} \right) \\ & + \frac{\varphi\dot{\varphi}}{\lambda(\nu + 8\pi\varphi^2)^2} \{ [(1 + 2\lambda)\nu + 4\pi(2 - 3\lambda)\varphi^2] \dot{\chi} + 4\pi(2 - 3\lambda)\varphi\dot{\varphi}\chi \} - \frac{2\nu\varphi}{(\nu + 8\pi\varphi^2)^2} [\mathcal{H}\dot{\varphi} + 4\pi\lambda(3w - 1)\rho a^2] \chi. \end{aligned} \quad (3.34)$$

Finally, the perturbed scalar field Eq. (3.17) gives

δφ equation

$$\ddot{\chi} + 2\mathcal{H}\dot{\chi} + k^2\chi + \frac{\dot{\varphi}}{2}\dot{h} = 4\pi\lambda \left(1 - 3\frac{\delta p}{\delta\rho} \right) \rho a^2 \delta. \quad (3.35)$$

IV. THE LENSING POTENTIAL

We assume the Newtonian gauge and neglecting anisotropic contributions from matter fields, $\sigma = 0$, the anisotropy Eq. (3.23) yields the following algebraic relation between the gravitational potentials and the scalar field perturbation

$$\Phi - \Psi = \frac{\chi}{D(\varphi)}, \quad (4.1)$$

where we have set

$$D(\varphi) = \frac{\nu + 8\pi\varphi^2}{8\pi\varphi}. \quad (4.2)$$

Equation (4.1) defines the slip χ between the Newtonian potentials and expresses the departure from standard

general relativity where the anisotropy equation is the simple equation $\Phi = \Psi$.

Since in (3.22) the only derivatives of the perturbed variables are encountered in the combination $\dot{\Phi} - \frac{\dot{\chi}}{2D}$, defining $\Phi_+ = \Phi - \frac{\chi}{2D}$, only the single derivative $\dot{\Phi}_+$ will remain. Due to (4.1) it is

$$\Phi_+ = \frac{\Phi + \Psi}{2}, \quad (4.3)$$

which is called lensing potential. This is responsible for such effects as the integrated Sachs-Wolfe effect in the CMB and weak lensing of distant galaxies. Due to Eq. (4.1), among the gravitational potentials Φ , Ψ and the scalar field perturbation χ , only two are independent quantities, which are given by Φ_+ , χ . The variables Φ_+ , χ are linear combinations of the gravitational potentials Φ , Ψ , and inversely

$$\Phi = \Phi_+ + \frac{\chi}{2D} \quad (4.4)$$

$$\Psi = \Phi_+ - \frac{\chi}{2D}. \quad (4.5)$$

We will transform the remaining gravitational equations (3.20) and (3.22) into a coupled system of first-order differential equations for Φ_+ , χ . These are the functions to be evolved along with the perturbations of the matter fields. This analysis will facilitate the numerical treatment of the equations and the interpretation of the results.

Starting with (3.22) we get, after the substitution (4.4), (4.5)

$$\Phi'_+ = -\left(1 + \frac{\varphi'}{2D}\right)\Phi_+ + \frac{1}{2D^2}\left(D' + \frac{\varphi'}{2}\right)\chi + \frac{4\pi\varphi'}{\lambda(\nu + 8\pi\varphi^2)^2}[\nu(1 + \lambda) + 4\pi(2 - 3\lambda)\varphi^2]\chi + \frac{4\pi}{kH\varphi}(1 + w)\rho av, \quad (4.6)$$

where, as mentioned, a prime denotes differentiation with respect to $\ln a$.

A suitable linear combination of Eq. (3.20) and (3.22) leads to an equation containing the comoving density perturbation

$$\Delta = \delta + \frac{3\mathcal{H}}{k}V, \quad (4.7)$$

where $V = (1 + w)v$. Using again (4.4) and (4.5) to convert everything into Φ_+ and χ , we finally get

$$\begin{aligned} \frac{\varphi'}{\lambda D}\chi' = & -\frac{8\pi\rho}{H^2}\Delta + 3\chi - \frac{4\pi(\nu - 24\pi\varphi^2)}{\lambda(\nu + 8\pi\varphi^2)^3}[\nu + 4\pi(2 - 3\lambda)\varphi^2]\varphi'^2\chi + \frac{8\pi}{\nu + 8\pi\varphi^2}\left\{\frac{3\nu\varphi'}{4\pi D} + 3\varphi^2 + \frac{3\varphi^2\varphi'}{2D} + \frac{2\varphi^2 D'\varphi'}{2D^2}\right. \\ & \left. - \frac{2 - 3\lambda}{2\lambda D}\varphi\varphi'\left(\frac{\varphi\varphi'}{2D} + \varphi' + 3\varphi\right) - \frac{\nu\varphi'}{8\pi\lambda D}\left[\frac{\varphi'}{2D} + 3(1 + \lambda)\right]\right\}\chi - \frac{3\varphi\varphi'}{D}\Phi_+' \\ & + \frac{8\pi\varphi'}{\nu + 8\pi\varphi^2}\left(\frac{2 - 3\lambda}{2\lambda D}\varphi^2\varphi' + \frac{\nu}{8\pi\lambda D}\varphi' - 3\varphi^2\right)\Phi_+ - \frac{2k^2\varphi}{a^2H^2}\Phi_+. \end{aligned} \quad (4.8)$$

We now have the tools to obtain the evolution of the linear perturbations in the complete Brans-Dicke theory. Equations (3.18), (3.19) can easily be expressed in terms of the lensing potential and primed derivatives. Equation (3.24) is the redundant equation. We will solve numerically the system of the first-order differential equations (3.18), (3.19), (4.6), and (4.8). This system is well-defined since the isotropic pressure δp can be considered negligible in the scales of interest. In principle δp could be substituted from Eq. (3.26), however this would bring unnecessary complexity due to the second derivatives of χ , so we do not follow this method. The remaining part of Eq. (3.26) can be checked for consistency in the end for the numerical solution obtained. However, in the subhorizon approximation of the next section the consistency of this equation will become manifest. In order to perform the numerical integration, we impose initial conditions on Φ_+ and χ at a redshift of $z_i = 1000$, as if we had minimal deviations from standard general relativity, i.e. $\Phi_{+i} = -1$ and $\chi_i = 0$. Since in GR the two Newtonian potentials remain constant in the initial era of evolution and the lensing potential is a combination of these potentials, it is reasonable to set $\Phi_{+i}' = 0$. Then, Eqs. (4.6) and (4.8) provide the initial velocity v_i of the matter perturbation and the initial comoving density perturbation Δ_i . Indeed, using (2.11) initially, we get the standard GR relations

$$v_i = \frac{2k}{3a_i H_i}\Phi_{+i} \quad (4.9)$$

$$\Delta_i = -\frac{2k^2}{3a_i^2 H_i^2}\Phi_{+i}. \quad (4.10)$$

We can see the evolution of the lensing potential Φ_+ and the slip χ in Figs. 3(a) and 3(b), respectively, for the CBD model. The first immediate observation is that the evolution of the linear perturbations in the complete Brans-Dicke theory (both the lensing potential and the slip) is scale-dependent, particularly at early-times. This is a general feature of modified gravity theories, and is in complete contrast to the scale-independent GR+ Λ CDM predictions. Indeed in GR, the absence of χ makes Eqs. (4.6) and (3.19) an autonomous system for Φ , $\hat{v} = v/k$, without containing k . Together with the above initial conditions $\Phi_i = -1$, $\hat{v}_i = 2\Phi_i/(3\mathcal{H}_i)$, which do not contain k as well, it arises that Φ , \hat{v} are scale-independent in GR, while (4.8) shows that δ is scale-dependent in GR. In CBD however, the existence of the last k -term in (4.8), as well as the kv term in (3.18), result in the scale-dependence of all perturbations.

Then, we have the oscillatory behavior of the slip between the Newtonian potentials, shown in Fig. 3(b). This is also observed in other (noninteracting) scalar-tensor theories such as metric $f(R)$ [50], or the hybrid metric-Palatini theory [51], and can be understood from Eq. (3.26) which is the equation of a damped harmonic oscillatory with a driving term. We observe these oscillations mainly at early-times, and they become more pronounced the smaller the scales (higher k 's) we consider, as these modes start

deep within the range of action of the additional force the scalar degree of freedom mediates. As in standard Brans-Dicke theory (with at most a constant potential), we have a massless scalar field. Hence, its effective Compton radius can include and impact even the largest scales (smallest k) we consider at early times. These oscillations could lead to instabilities at early-times. For instance, in metric $f(R)$, the oscillations in the gravitational potentials manifest in the perturbation of the metric Ricci scalar δR , leading to a possible overproduction of new massive scalar particles in the very early Universe [52]. A more detailed study on this is, however, beyond the scope of the current work.

As the cosmological evolution continues, the oscillations in χ get progressively damped by the Hubble friction term in Eq. (3.26), and they eventually get smoothed and unnoticeable toward the present. As we approach $a = 1$, we see that the equilibrium position of χ is shifted from zero to a positive value, and shows a tendency to increase. This is due to the driving term in Eq. (3.26), which tries to displace χ from the equilibrium position set by the initial conditions. Hence, as δ grows, the driving term will become more important, and its overall effect will be more significant the larger the value of λ is.

Lastly, we have the lensing potential Φ_+ in Fig. 3(a). We have again the distinct effect of the scale-dependent oscillations at early times that propagate from the evolution in χ . Such rapid oscillations in Φ_+ can contribute to a significant early-times integrated Sachs-Wolfe (eISW) effect, which could impact the CMB as seen in Ref. [53] for instance. Furthermore, we also have a noticeable departure from standard GR+ Λ CDM toward the present. We can see in Fig. 3(a) that the absolute value of the lensing potential exhibits a distinct growing tendency at late-times. In the standard cosmological model, with the onset of cosmic

acceleration, the lensing potential decays due to the expanding background. What we see in CBD is that, despite having accelerating background solutions, $|\Phi_+|$ actually grows as we approach $a = 1$, yielding a late-times integrated Sachs-Wolfe (IISW) effect opposite to that of Λ CDM. This should produce a noticeable impact on the larger scales of the CMB, which might cause difficulties with current observations of the IISW [54–56].

Note also from Eqs. (4.4), (4.5), and Fig. 3 that the Newtonian potentials Φ , Ψ oscillate around -1 at early times. Although these potentials normally acquire negative values due to the attractive character of gravity, however, it can be seen that Ψ passes to positive values at late times. This late-times behaviour of Ψ will become significant in Sec. VI, where the behaviour of δ will be studied.

V. SUBHORIZON APPROXIMATION

We now consider wave modes that are deep within the Hubble radius such that $k \gg aH$. In this limit, we adopt the quasistatic approximation, discarding time derivatives of perturbations when compared to their spatial variation. This is generally a good approximation for scalar-tensor theories on small scales [57]. In practice, this allows one to keep the terms proportional to $k^2/(a^2H^2)$, as well as those related to the matter perturbation δ and ϖ , and is known as the subhorizon approximation [58,59]. Equation (3.20) becomes

$$\Phi = -\frac{4\pi a^2}{\varphi k^2} \rho \delta + \frac{4\pi\varphi}{\nu + 8\pi\varphi^2} \chi. \quad (5.1)$$

Therefore, Eq. (3.20), which gave the differential equation (4.8) for χ , has now become an algebraic equation. Equation (3.23) coincides with equation (4.1) for the

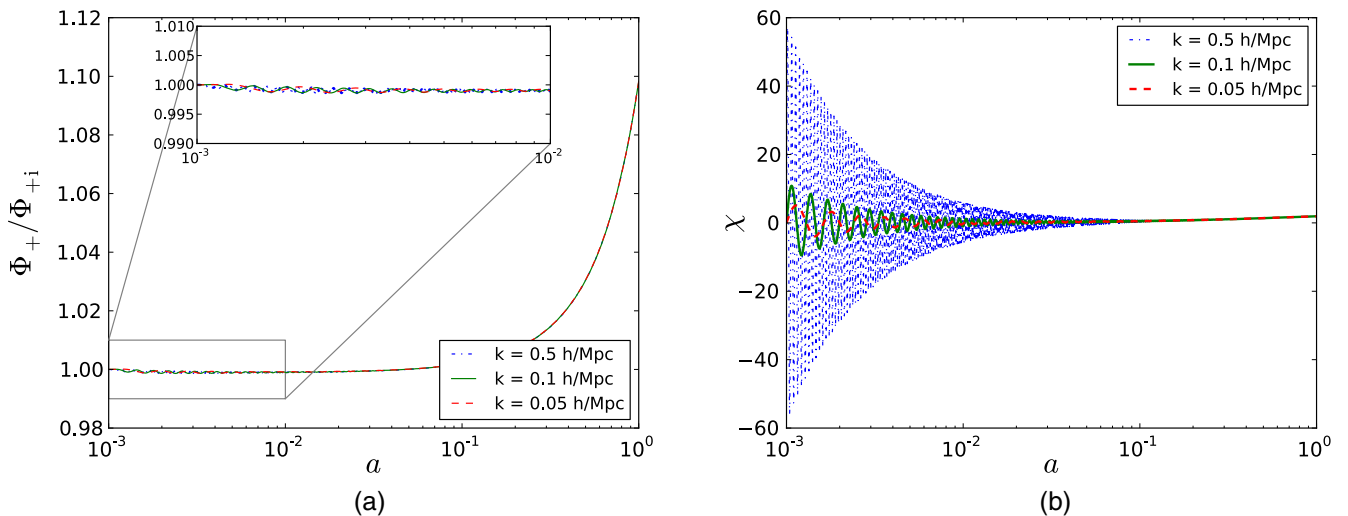


FIG. 3. We plot the evolution of the lensing potential Φ_+ and the slip χ between the Newtonian potentials as a function of scale factor for different k (h/Mpc) scales, using the CBD model.

slip. Also the complicated equation (3.24) gets the simple algebraic form

$$\Phi - \Psi = \frac{8\pi\varphi}{\nu + 8\pi\varphi^2}\chi + \frac{12\pi a^2}{\varphi k^2}\varpi. \quad (5.2)$$

Due to Eq. (4.1), Eq. (5.2) gives $\varpi = 0$, so in the subhorizon approximation our previous assumption of negligible isotropic pressure perturbation is verified. This means that in the context of the present approximation the $i - i$ and $i - j$ ($i \neq j$) equations coincide if $\varpi = 0$, and they provide information for the potential Ψ . The differential equation (3.26) becomes

$$\chi = 4\pi\lambda \frac{a^2}{k^2}\rho\delta - 12\pi\lambda \frac{a^2}{k^2}\varpi, \quad (5.3)$$

where $\varpi = 0$ has to be set. Therefore, we see a proportionality between the slip χ and the matter perturbation δ . Finally, Eq. (3.22) or the lensing potential equation (4.6) does not accept any simplification and is the redundant equation in this approximation, which should be satisfied on shell.

From Eqs. (5.1) and (5.3) we can express Φ in terms of δ as

$$\frac{k^2}{a^2}\Phi = -\frac{4\pi}{\varphi} \left(\frac{\nu + 8\pi\varphi^2(1 - \lambda/2)}{\nu + 8\pi\varphi^2} \right) \rho\delta. \quad (5.4)$$

Then, from Eq. (5.2) we get Ψ as

$$\frac{k^2}{a^2}\Psi = -\frac{4\pi}{\varphi} \left(\frac{\nu + 8\pi\varphi^2(1 + \lambda/2)}{\nu + 8\pi\varphi^2} \right) \rho\delta, \quad (5.5)$$

and we write again Eq. (5.3) for completeness

$$\chi = 4\pi\lambda \frac{a^2}{k^2}\rho\delta. \quad (5.6)$$

Equations (5.4), (5.5), and (5.6) express algebraically the gravitational and scalar field perturbations in terms of the matter density perturbation δ . This δ is given by the system of equations (3.18) and (3.19) after substitution of (5.4), (5.5), and (5.6). In the next section, we will derive an autonomous second-order differential equation for δ within the subhorizon approximation. Note also from Eqs. (5.4), (5.5), and (5.6) the proportionality of Φ , Ψ to χ , in agreement with the late-times behaviours derived numerically in the previous section without any approximation.

Lastly, we can relate from the above expressions the lensing potential Φ_+ in the subhorizon approximation to the scalar-field perturbation as

$$\Phi_+ = -\frac{1}{\lambda\varphi}\chi. \quad (5.7)$$

This equation also coincides with the subhorizon limit of the slip equation (4.8), where a term proportional to v/k should be ignored in this limit [this is due to that ignoring the various terms in (4.8) means from (4.6) ignoring the term v/k]. From Eq. (5.7) we can anticipate that if χ grows at late-times, then Φ_+ will follow that behavior, increasing in absolute amplitude, in agreement with Fig. 3(a). The scale-independence of χ at late-times, shown in Fig. 3(b) and explained in the next section, implies also the same independence for Φ_+ , Φ , Ψ . This is consistent with the nonmassive Brans-Dicke theory [60], and contrasts, for instance, with metric $f(R)$ theories [50]. This is the reason why we are not able to resolve the differences in the evolution of the lensing potential and χ in Fig. 3 for the different k scales when we approach the present time.

We can now write the two functions that are commonly used to parametrize deviations from general relativity in modified theories of gravity, $\mu(a, k)$ and $\gamma(a, k)$. The former defines the relation between the Newtonian potential Ψ and the matter density perturbation, while the latter parametrizes the ratio between the gravitational potentials, such as [61,62]

$$\frac{k^2}{a^2}\Psi = -4\pi\mu(a, k)\rho\delta, \quad (5.8)$$

$$\frac{\Phi}{\Psi} = \gamma(a, k). \quad (5.9)$$

Hence, for the complete Brans-Dicke theory, these functions will take the form

$$\mu_{\text{CBD}}(a, k) = \frac{1}{\varphi} \frac{\nu + 8\pi\varphi^2(1 + \lambda/2)}{\nu + 8\pi\varphi^2}, \quad (5.10)$$

$$\gamma_{\text{CBD}}(a, k) = \frac{\nu + 8\pi\varphi^2(1 - \lambda/2)}{\nu + 8\pi\varphi^2(1 + \lambda/2)}, \quad (5.11)$$

which recover the known results for standard massless Brans-Dicke in the limit of $\nu = 0$ [60]

$$\mu_{\nu=0}(a, k) = \frac{2\omega_{\text{BD}} + 4}{2\omega_{\text{BD}} + 3}, \quad (5.12)$$

$$\gamma_{\nu=0}(a, k) = \frac{\omega_{\text{BD}} + 1}{\omega_{\text{BD}} + 2}. \quad (5.13)$$

VI. GROWTH RATE

The equations for matter perturbations (3.18) and (3.19) in the matter era with $\sigma = \varpi = 0$ take the following form (without making use of the approximation on subhorizon scales)

$$\ddot{\delta} + kv - 3\dot{\Phi} = \frac{\nu}{\varphi(\nu + 8\pi\varphi^2)}\dot{\chi} - \frac{\nu(\nu + 24\pi\varphi^2)}{\varphi^2(\nu + 8\pi\varphi^2)^2}\dot{\varphi}\chi \quad (6.1)$$

$$\dot{v} + \mathcal{H}v - k\Psi = 0. \quad (6.2)$$

We differentiate (6.1) once more and eliminate \dot{v} , v from (6.1) and (6.2) to find the equation of motion for δ

$$\begin{aligned} &\ddot{\delta} + \mathcal{H}\dot{\delta} + k^2\Psi - 3\ddot{\Phi} - 3\mathcal{H}\dot{\Phi} \\ &= \frac{1}{a} \left[\frac{\nu a}{\varphi(\nu + 8\pi\varphi^2)}\dot{\chi} - \frac{\nu(\nu + 24\pi\varphi^2)a}{\varphi^2(\nu + 8\pi\varphi^2)^2}\dot{\varphi}\chi \right]. \end{aligned} \quad (6.3)$$

Now the subhorizon approximation can be implemented and Eq. (6.3) gets simplified as

$$\ddot{\delta} + \mathcal{H}\dot{\delta} + k^2\Psi = 0. \quad (6.4)$$

Converting to e-folding time $\ln a$ we get

$$\delta'' + \left(\frac{\mathcal{H}'}{\mathcal{H}} + 1 \right) \delta' + \frac{k^2}{\mathcal{H}^2} \Psi = 0. \quad (6.5)$$

Using Eq. (5.5) to replace Ψ we obtain

$$\delta'' + \left(\frac{\mathcal{H}'}{\mathcal{H}} + 1 \right) \delta' - \frac{4\pi\nu + 4\pi(2 + \lambda)\varphi^2}{\mathcal{H}^2 \varphi(\nu + 8\pi\varphi^2)} \rho a^2 \delta = 0. \quad (6.6)$$

The second order differential equation (6.6) for the dynamics of the linear matter perturbations δ can also be written as

$$f' + f^2 + \left(\frac{\mathcal{H}'}{\mathcal{H}} + 1 \right) f - \frac{4\pi\nu + 4\pi(2 + \lambda)\varphi^2}{\mathcal{H}^2 \varphi(\nu + 8\pi\varphi^2)} \rho a^2 = 0, \quad (6.7)$$

where $f = \frac{d \ln \delta}{d \ln a}$ is the linear growth rate. The modified gravitational coupling predicted by the CBD theory through $\mu_{\text{CBD}}(a, k)$ will lead to a growth history that is different than that of an effective dark energy model within GR that exhibits the same expansion history as our complete Brans-Dicke model.

Equation (6.6) defines an autonomous differential equation for the quantity $\hat{\delta} = \delta/k^2$. No k -dependence is present in this equation for $\hat{\delta}$. Moreover, from the initial conditions (4.9) and (4.10) we get $\hat{\delta} = -2\Phi_{+i}/(3\mathcal{H}_i^2)$, which also does not depend on k . This initial condition also arises from the subhorizon Eqs. (5.7) and (5.6) with the use of (2.11). Since both the differential equation and the initial condition of $\hat{\delta}$ do not depend on k , thus $\hat{\delta}$ is scale-independent, which means that δ is proportional to k^2 in the subhorizon limit (the same is true in the subhorizon limit of GR). From Eq. (5.6), we obtain that χ is scale-independent in this approximation, in agreement with the late-times behaviour

of Fig. 3(b). Thus, all Φ_+ , Φ , Ψ are scale-independent in this limit. Finally, since knowing $\hat{\delta}$ means from (5.5) that Ψ is known and scale-independent, thus Eq. (6.2) is converted into an autonomous differential equation for $\hat{v} = v/k$ which does not depend on k . Additionally, the initial condition (4.9) is $\hat{v}_i = 2\Phi_{+i}/(3\mathcal{H}_i)$, which also does not depend on k . Therefore, \hat{v} is scale-independent and v depends linearly on k in the subhorizon approximation (this is also true in GR, but at all times).

In Fig. 4 we plot for recent redshifts the numerical evolution of $f\sigma_8(z)$, also known as growth rate, with the amplitude of fluctuations $\sigma_8(z)$ given by

$$\sigma_8(z) = \sigma_8^0 \frac{\delta(z, k)}{\delta(0, k)}, \quad (6.8)$$

where the current value of σ_8 can be estimated through the cosmic microwave background [43], weak-lensing [63], or galaxy clustering [64]. On the other hand, $f\sigma_8$ can be extracted from redshift space distortions (RSD) observations as a function of redshift. The most recent $f\sigma_8$ data points available were used in Fig. 4, and can be consulted in Table I. The plot of Fig. 4 has been made using the exact equations discussed in Sec. IV, and not the approximated Eq. (6.7).

We can see in this figure that the CBD theory predicts less growth than Λ CDM, and could potentially provide a better fit to existent RSD data than the concordance cosmological model. This may seem counterintuitive given that, in Sec. IV, we concluded that the lensing potential Φ_+ exhibited a distinct late-time growth as the slip between the gravitational potentials also grew at late-times. Since the scale used in Fig. 4 is certainly subhorizon at low redshifts, the decrease of $f\sigma_8$ or also of f , compared to Λ CDM, can be explained from the last term in Eq. (6.7). The effective

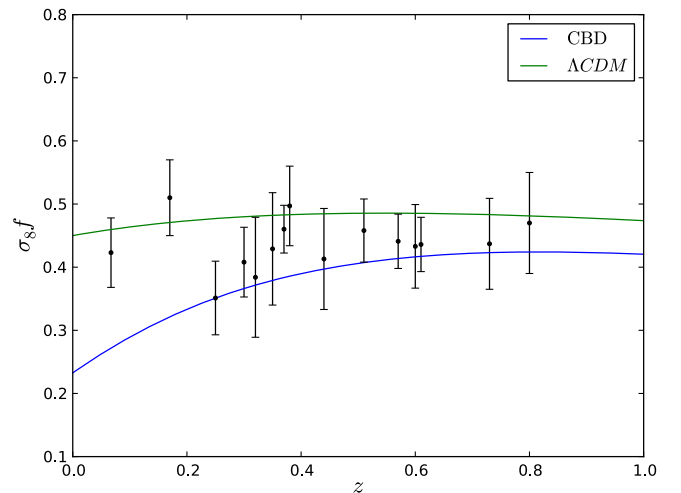


FIG. 4. We plot $f\sigma_8$ for the CBD model against Λ CDM. The data points used can be seen in Table I. The parameters used were $\lambda = 1$, $\nu = -100$ and $\hat{\Omega}_m = 0.17$, $\varphi_i = 0.029$. We have taken $\sigma_8^0 = 0.83$, as measured by the Planck collaboration [43].

TABLE I. RSD $f\sigma_8$ measurements from various sources, used in Fig. 4.

Survey	z	$\sigma_8 f(z)$	Source
6dFGRS	0.067	0.423 ± 0.055	Beutler <i>et al.</i> (2012) [65]
LRG-200	0.25	0.3512 ± 0.0583	Samushia <i>et al.</i> (2012) [66]
	0.37	0.4602 ± 0.0378	
BOSS	0.30	0.408 ± 0.0552	Tojeiro <i>et al.</i> (2012) [67]
	0.60	0.433 ± 0.0662	Alam <i>et al.</i> (2016) [68]
	0.38	0.497 ± 0.063	
	0.51	0.458 ± 0.050	
	0.61	0.436 ± 0.043	
WiggleZ	0.44	0.413 ± 0.080	Blake (2011) [69]
	0.73	0.437 ± 0.072	
Vipers	0.8	0.47 ± 0.08	De la Torre <i>et al.</i> (2013) [70]
2dFGRS	0.17	0.51 ± 0.06	Percival <i>et al.</i> (2004) [71,72]
LRG	0.35	0.429 ± 0.089	Chuang and Wang (2013)
			[73]
LOWZ	0.32	0.384 ± 0.095	Chuang <i>et al.</i> (2013) [74]
CMASS	0.57	0.441 ± 0.043	Samushia <i>et al.</i> (2013) [75]

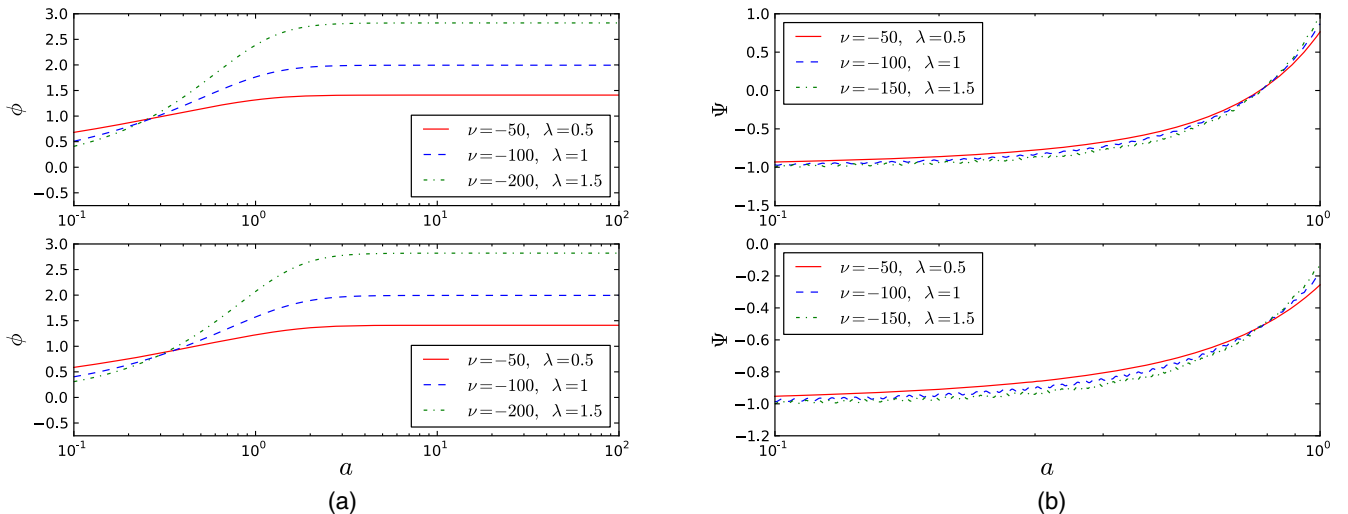
gravitational coupling concerning the perturbations is given from (6.7) as $G_{\text{eff}} = \frac{\nu+4\pi(2+\lambda)\varphi^2}{\varphi(\nu+8\pi\varphi^2)}$, and it can be seen that G_{eff} passes from positive to negative values recently. This change of sign happens when the scalar field crosses the critical value $\varphi_c = \sqrt{|\nu|/[4\pi(2+\lambda)]}$, and it is $\varphi_c < \varphi_\infty$ as long as $\lambda > 0$. For Λ CDM or for BD, the corresponding G_{eff} 's are positive. Therefore, as φ grows toward the present, f' in the CBD theory acquires a negative contribution (or before that, a decaying positive contribution) due to G_{eff} , providing less growth. Similarly, the equation governing $f\sigma_8$ in the subhorizon approximation arises from (6.7) as

$$(f\sigma_8)' + \left(\frac{\mathcal{H}'}{\mathcal{H}} + 1\right)f\sigma_8 + \frac{\sigma_8^0}{\delta(0,k)} \frac{k^2}{\mathcal{H}^2} \Psi = 0, \quad (6.9)$$

where the Newtonian potential Ψ from (5.5) is proportional to G_{eff} and of opposite sign. A recent negative G_{eff} gives a positive Ψ , as already known, and decreases $f\sigma_8$. A similar behavior in G_{eff} was observed in a specific nonlocal model of modified gravity that also lead to a prediction of less growth than Λ CDM [76].

We have tested numerically that, as long as one requires $\Omega_{\text{DE}}^0 \approx 0.7$, the above change in sign of G_{eff} or Ψ close to the present persists, independently of the parameters or the initial conditions of the background evolution, even set at different redshifts. We have actually found very special values of the parameters (with $\lambda < 0$) and initial conditions, consistent with $\Omega_{\text{DE}}^0 \approx 0.7$, such that $G_{\text{eff}}^0 > 0$, however, the whole cosmology arising is physically unacceptable. Also, G_{eff} can remain permanently positive if the requirement of background viability is relaxed and Ω_{DE}^0 is set to a value of approximately 1/2. We can not, for now, provide a definite proof on the inevitability of the change of sign in G_{eff} for reasonable evolutions of the CBD theory; however it seems that the scalar field evolves toward φ_∞ as we progress into the far future, and before reaching the present-time, will already have crossed the critical value φ_c . In Fig. 5, we plot the evolution of the scalar field ϕ (background part only) as a function of the scale factor a (which we extend beyond $a = 1$) for different parameters λ and ν , together with the evolution of Ψ . As we can see, the crossing in Ψ is inevitable, unless one relaxes the requirement of having $\Omega_{\text{DE}}^0 \approx 0.7$ today. Only when we take $\Omega_{\text{DE}}^0 \approx 0.5$ is the crossing in Ψ not verified, as the scalar field tends to same asymptotic value more slowly.

Negative values of G_{eff} is a fundamental issue and may jeopardize the viability of the theory on the smallest scales;


 FIG. 5. We plot the evolution of the scalar field ϕ (background part only) and the Newtonian potential Ψ as a function of scale factor, for the CBD model. On the top plots, we have $\Omega_{\text{DE}}^0 \approx 0.7$, while on the bottom plots we require $\Omega_{\text{DE}}^0 \approx 0.5$.

however, this does not mean that the CBD theory should be ruled out immediately. First, it is possible that the gravitational constant that controls the gravitational effects in a static spherically symmetric configuration around a central mass is unrelated to the above G_{eff} . This issue can be resolved if local solutions are found and a parameterized post-Newtonian analysis is performed. There could also be a screening mechanism ensuring the suppression of the additional interaction mediated by the theory on the smallest scales and, hence, hiding any evidence of this change of sign in G_{eff} . Another option could be that the theory does not couple to baryons, and hence only impact dark matter, allowing it to modify galactic dynamics without affecting ordinary matter and passing laboratory tests of gravity. Lastly, there is the possibility of considering a potential $V(\phi)$ that does not have to be dominant today, but could provide the necessary contribution to the dark energy density that would prevent the scalar field crossing the critical value that changes the sign of G_{eff} . It would also be interesting to perform a complete dynamical analysis of the equations of motion of the theory, since this would allow to make a more definitive statement on the behavior of G_{eff} and, eventually, find background attractor solutions that could avoid this problem altogether.

VII. CONCLUSIONS

In this work, we focused on one of three generalizations of the standard Brans-Dicke gravity (BD), named as complete Brans-Dicke theories (CBD) [36]. These were derived at the level of the field equations by analyzing exhaustively the Bianchi identities, while maintaining the BD scalar field wave equation and relaxing the standard matter conservation.

For this particular model, which for brevity we also refer to as CBD, there is one new parameter ν that mediates the interaction between the dark sectors. It had been previously shown that, for negative values of this parameter, the theory was able to produce accelerating cosmological solutions today without the presence of a potential $V(\phi)$ [38]. Here, we have extended the applicability of these solutions to high redshifts, which, as we show in Sec. II, yield a stable matter domination regime that is gradually overtaken by the dark energy component to yield acceleration today. Moreover, we obtain a nice fit to the low-redshift supernovae data. For our background solutions, we assume slow-roll initial conditions, with the initial value of the scalar field being found by requiring $\Omega_{\text{DE}} \approx 0.7$ today.

We then study the evolution of linear perturbations in the CBD theory in order to understand the impact it can have on the large scale structure of the Universe we observe. We present the full set of perturbed gravitational equations in both the Newtonian and synchronous gauges. One feature that becomes immediately obvious, and is transversal to most modified gravity theories, is the dynamical anisotropy

between the gravitational potentials, dependent on the perturbation χ of the scalar field.

In particular, χ evolves according to a damped harmonic oscillator subjected to an external force proportional to the matter perturbation δ . At late-times, as we show in Sec. IV, after the oscillations have been damped out, χ is pushed toward larger values relatively to its equilibrium initial position which we set to zero. In turn, this is manifested in the lensing potential Φ_+ which exhibits an unusual growth at late-times. Hence, Φ_+ not only resists the expanding background, but does increasing in amplitude, in a clear departure from Λ CDM, where the perturbations are expected to decay once Λ starts to dominate. This behavior becomes clear looking at the subhorizon quasistatic approximation for the evolution of the Newtonian potentials, which we present in Sec. V. Then, the lensing potential is directly proportional to χ , and hence follows its late-time behavior, growing as we approach $a = 1$.

Another interesting feature is that the evolution of all perturbations in the CBD theory is scale-dependent at early times. At late-times the gravitational potentials and the scalar field perturbation become scale-independent; what can be explained through the subhorizon approximation and also be observable in our numerical results. This is verified in nonmassive standard Brans-Dicke gravity as well [60].

We have also studied the evolution of the growth rate for the complete Brans-Dicke theory. We have concluded that the CBD theory predicts less growth than Λ CDM, and could produce a better fit to existent $f\sigma_8(z)$ data from RSD observations. This fact is clearly explained in the subhorizon approximation, where the behaviour of $f\sigma_8(z)$ is controlled by the time-time Newtonian potential Ψ . Contrary to the behavior of the lensing potential, Ψ passes from negative to positive values recently, and hence, as the scalar field grows in time, the theory predicts less growth than Λ CDM. However, in parallel with the sign change of Ψ in the subhorizon scales, the effective gravitational constant G_{eff} for the perturbations also changes sign and becomes negative recently. This effect seems to persist independently of the choice of the parameters or the initial conditions of any reasonable background evolution, and may jeopardize the validity of the theory on the smallest scales. It is premature to decide on this before local spherically symmetric solutions are found and the existence of screening mechanisms is investigated that might suppress the additional interaction mediated by the theory in order to pass the stringent solar-system tests of gravity. Other options would be the decoupling of baryons from the theory which would alleviate the small scale constraints on the theory, or the existence of a potential preventing the sign change of G_{eff} . Finally, the study of the background attractor solutions through a dynamical system analysis should allow a more decisive statement on the behavior of G_{eff} .

ACKNOWLEDGMENTS

The authors would like to thank Emmanuel Saridakis for helpful discussions about the background solutions of the complete Brans-Dicke theory. We also thank Luca Amendola and Valeria Pettorino for helpful discussions and comments. The work of N. A. L. is supported by the Deutsche Forschungsgemeinschaft (DFG) through the Transregional Research Center TRR33 The Dark Universe.

**APPENDIX: JORDAN FRAME
PERTURBATION EQUATIONS**

We present here some perturbed geometric quantities used for deriving the perturbed equations of motion. As for the Christoffel symbols we have

$$\delta\Gamma^0_{00} = \dot{A}Y, \quad \delta\Gamma^0_{0i} = -(kA + \mathcal{H}B)Y_i \quad (\text{A1})$$

$$\begin{aligned} \delta\Gamma^0_{ij} = & \left(-2\mathcal{H}A + \frac{k}{3}B + 2\mathcal{H}H_L + \dot{H}_L \right) \delta_{ij}Y \\ & + (-kB + 2\mathcal{H}H_T + \dot{H}_T)Y_{ij} \end{aligned} \quad (\text{A2})$$

$$\delta\Gamma^i_{00} = -(kA + \dot{B} + \mathcal{H}B)Y^i \quad (\text{A3})$$

$$\delta\Gamma^i_{0j} = \dot{H}_L \delta^i_j Y + \dot{H}_T Y^i_j \quad (\text{A4})$$

$$\begin{aligned} \delta\Gamma^i_{jk} = & -kH_L(\delta^i_j Y_k + \delta^i_k Y_j - \delta_{jk}Y^i) + \mathcal{H}B\delta_{jk}Y^i \\ & + H_T(Y^i_{j,k} + Y^i_{k,j} - Y_{jk}{}^i). \end{aligned} \quad (\text{A5})$$

Indices in Y_i , Y_{ij} are raised with δ^{ij} . The perturbed Ricci tensor and Ricci scalar are

$$\begin{aligned} \delta R = & \frac{2}{a^2} \left[-6\frac{\ddot{a}}{a}A - 3\mathcal{H}\dot{A} + k^2A + k\dot{B} + 3k\mathcal{H}B \right. \\ & \left. + 9\mathcal{H}\dot{H}_L + 3\ddot{H}_L + 2k^2\left(H_L + \frac{H_T}{3}\right) \right] Y \end{aligned} \quad (\text{A6})$$

$$\delta R_{00} = -[k^2A - 3\mathcal{H}\dot{A} + k(\dot{B} + \mathcal{H}B) + 3\ddot{H}_L + 3\mathcal{H}\dot{H}_L]Y \quad (\text{A7})$$

$$\delta R_{0i} = \left[-\left(\frac{\ddot{a}}{a} + \mathcal{H}^2\right)B - 2k\mathcal{H}A + 2k\dot{H}_L + \frac{2}{3}k\dot{H}_T \right] Y_i \quad (\text{A8})$$

$$\begin{aligned} \delta R_{ij} = & \left[-2\left(\frac{\ddot{a}}{a} + \mathcal{H}^2\right)A - \mathcal{H}\dot{A} + \frac{k^2}{3}A + \frac{k}{3}(\dot{B} + 5\mathcal{H}B) \right. \\ & \left. + \dot{H}_L + 5\mathcal{H}\dot{H}_L + 2\left(\frac{\ddot{a}}{a} + \mathcal{H}^2\right)H_L \right. \\ & \left. + \frac{4k^2}{3}\left(H_L + \frac{H_T}{3}\right) \right] \delta_{ij}Y + \left[-k^2A - k(\dot{B} + \mathcal{H}B) \right. \\ & \left. + \dot{H}_T + \mathcal{H}\dot{H}_T + 2\left(\frac{\ddot{a}}{a} + \mathcal{H}^2\right)H_T - k^2\left(H_L + \frac{H_T}{3}\right) \right. \\ & \left. + \mathcal{H}(\dot{H}_T - kB) \right] Y_{ij}. \end{aligned} \quad (\text{A9})$$

The perturbations of the scalar field derivatives, due to $\delta g_{\mu\nu}$ and $\delta\phi$, are given by the expressions

$$\delta(\nabla_\mu\nabla_\nu\phi) = \nabla_\mu\nabla_\nu(\delta\phi) - \delta\Gamma^\lambda_{\mu\nu}\partial_\lambda\phi \quad (\text{A10})$$

$$\delta(\nabla^\mu\nabla_\nu\phi) = \nabla^\mu\nabla_\nu(\delta\phi) + \delta g^{\mu\lambda}\nabla_\lambda\nabla_\nu\phi - g^{\mu\lambda}\delta\Gamma^\kappa_{\lambda\nu}\partial_\kappa\phi, \quad (\text{A11})$$

where $\delta(\nabla_\mu\nabla_\nu\phi) = \nabla_\mu\nabla_\nu\phi - \bar{\nabla}_\mu\bar{\nabla}_\nu\phi$, $\delta(\nabla^\mu\nabla_\nu\phi) = g^{\mu\lambda}\nabla_\nu\nabla_\lambda\phi - \bar{g}^{\mu\lambda}\bar{\nabla}_\nu\bar{\nabla}_\lambda\phi$, $\bar{\nabla}$ denotes the covariant derivative with respect to the perturbed metric $g_{\mu\nu}$, ∇ denotes the covariant derivative with respect to the background metric $\bar{g}_{\mu\nu}$ and $\phi = \varphi + \delta\phi$. Since $\delta\phi = \chi(t)Y$, we get

$$\delta(\nabla_0\nabla_i\phi) = [-k\dot{\chi} + k\mathcal{H}\chi + \dot{\phi}(kA + \mathcal{H}B)]Y_i \quad (\text{A12})$$

$$\delta(\nabla_0\nabla_0\phi) = (\ddot{\chi} - \mathcal{H}\dot{\chi} - \dot{\phi}\dot{A})Y \quad (\text{A13})$$

$$\begin{aligned} \delta(\nabla_i\nabla_j\phi) = & \left[-\mathcal{H}\dot{\chi} - \frac{k^2}{3}\chi \right. \\ & \left. + \dot{\phi}\left(2\mathcal{H}A - \frac{k}{3}B - 2\mathcal{H}H_L - \dot{H}_L\right) \right] \delta_{ij}Y \\ & + [k^2\chi + \dot{\phi}(kB - 2\mathcal{H}H_T - \dot{H}_T)]Y_{ij} \end{aligned} \quad (\text{A14})$$

$$\delta(\nabla^0\nabla_0\phi) = \frac{1}{a^2}(-\ddot{\chi} + \mathcal{H}\dot{\chi} + 2\ddot{\phi}A - 2\dot{\phi}\mathcal{H}A + \dot{\phi}\dot{A})Y \quad (\text{A15})$$

$$\delta(\nabla^0\nabla_i\phi) = \frac{1}{a^2}(k\dot{\chi} - k\mathcal{H}\chi - k\dot{\phi}A)Y_i \quad (\text{A16})$$

$$\begin{aligned} \delta(\nabla^i\nabla_j\phi) = & \frac{1}{a^2}[k^2\chi + \dot{\phi}(kB - \dot{H}_T)]Y^i_j \\ & + \frac{1}{a^2}\left[-\mathcal{H}\dot{\chi} - \frac{k^2}{3}\chi + \dot{\phi}\left(2\mathcal{H}A - \frac{k}{3}B - \dot{H}_L\right) \right] \delta^i_j Y \end{aligned} \quad (\text{A17})$$

$$\delta(\nabla^i\nabla_i\phi) = \frac{1}{a^2}[-3\mathcal{H}\dot{\chi} - k^2\chi + \dot{\phi}(6\mathcal{H}A - kB - 3\dot{H}_L)]Y. \quad (\text{A18})$$

- [1] A. G. Riess *et al.*, *Astron. J.* **116**, 1009 (1998).
- [2] S. Perlmutter *et al.*, *Astrophys. J.* **517**, 565 (1999).
- [3] T. Padmanabhan, *Phys. Rep.* **380**, 235 (2003).
- [4] C. H. Brans and R. H. Dicke, *Phys. Rev.* **124**, 925 (1961).
- [5] A. Nicolis, R. Rattazzi, and E. Trincherini, *Phys. Rev. D* **79**, 064036 (2009).
- [6] T. P. Sotiriou and V. Faraoni, *Rev. Mod. Phys.* **82**, 451 (2010).
- [7] G. W. Horndeski, *Int. J. Theor. Phys.* **10**, 363 (1974).
- [8] L. Lombriser and N. A. Lima, *Phys. Lett. B* **765**, 382 (2017).
- [9] T. Clifton, P. G. Ferreira, A. Padilla, and C. Skordis, *Phys. Rep.* **513**, 1 (2012).
- [10] A. Joyce, L. Lombriser, and F. Schmidt, *Annu. Rev. Nucl. Part. Sci.* **66**, 95 (2016).
- [11] S. Nojiri and S. D. Odintsov, *Phys. Rep.* **505**, 59 (2011).
- [12] C. M. Will, *Living Rev. Relativ.* **9**, 3 (2006).
- [13] B. Bertotti, L. Iess, and P. Tortora, *Nature (London)* **425**, 374 (2003).
- [14] Y.-C. Li, F.-Q. Wu, and X. Chen, *Phys. Rev. D* **88**, 084053 (2013).
- [15] A. Avilez and C. Skordis, *Phys. Rev. Lett.* **113**, 011101 (2014).
- [16] N. Banerjee and D. Pavon, *Phys. Rev. D* **63**, 043504 (2001).
- [17] A. A. Sen, S. Sen, and S. Sethi, *Phys. Rev. D* **63**, 107501 (2001).
- [18] O. Bertolami and P. J. Martins, *Phys. Rev. D* **61**, 064007 (2000).
- [19] M. K. Mak and T. Harko, *Europhys. Lett.* **60**, 155 (2002).
- [20] S. Sen and A. A. Sen, *Phys. Rev. D* **63**, 124006 (2001).
- [21] W. Chakraborty and U. Debnath, *Int. J. Theor. Phys.* **48**, 232 (2009).
- [22] J. P. Uzan, *Phys. Rev. D* **59**, 123510 (1999).
- [23] N. Bartolo and M. Pietroni, *Phys. Rev. D* **61**, 023518 (1999).
- [24] A. R. Liddle and R. J. Scherrer, *Phys. Rev. D* **59**, 023509 (1998).
- [25] C. Santos and R. Gregory, *Ann. Phys. (N.Y.)* **258**, 111 (1997).
- [26] O. Bertolami, F. G. Pedro, and M. L. Delliou, *Phys. Lett. B* **654**, 165 (2007).
- [27] A. A. Costa, X. D. Xu, B. Wang, E. G. M. Ferreira, and E. Abdalla, *Phys. Rev. D* **89**, 103531 (2014).
- [28] S. del Campo, R. Herrera, and D. Pavon, *Phys. Rev. D* **91**, 123539 (2015).
- [29] L. Amendola, *Phys. Rev. D* **60**, 043501 (1999).
- [30] W. Zimdahl and D. Pavon, *Gen. Relativ. Gravit.* **36**, 1483 (2004).
- [31] T. Clifton and J. D. Barrow, *Phys. Rev. D* **73**, 104022 (2006).
- [32] L. L. Smalley, *Phys. Rev. D* **9**, 1635 (1974).
- [33] O. Bertolami and P. J. Martins, *Phys. Rev. D* **61**, 064007 (2000).
- [34] S. Das and N. Banerjee, *Phys. Rev. D* **78**, 043512 (2008).
- [35] W. Chakraborty and U. Debnath, *Int. J. Theor. Phys.* **48**, 232 (2009).
- [36] G. Kofinas, *Ann. Phys. (Amsterdam)* **376**, 425 (2017).
- [37] G. Kofinas and M. Tsoukalas, *Eur. Phys. J. direct A* **C76**, 686 (2016).
- [38] G. Kofinas, E. Papantonopoulos, and E. N. Saridakis, *Classical Quantum Gravity* **33**, 155004 (2016).
- [39] T. Abbott *et al.* (D. E. S. Collaboration), arXiv:astro-ph/0510346.
- [40] K. S. Dawson *et al.*, *Astron. J.* **151**, 44 (2016).
- [41] R. Laureijs *et al.*, arXiv:1110.3193.
- [42] K. Koyama, *Rep. Prog. Phys.* **79**, 046902 (2016).
- [43] P. A. R. Ade *et al.* (Planck Collaboration), *Astron. Astrophys.* **594**, A13 (2016).
- [44] W. Cardona, M. Kunz, and V. Pettorino, *J. Cosmol. Astropart. Phys.* **03** (2017) 056.
- [45] A. G. Riess *et al.*, *Astrophys. J.* **826**, 56 (2016).
- [46] A. G. Riess, L. Macri, S. Casertano, H. Lampeitl, H. C. Ferguson, A. V. Filippenko, S. W. Jha, W. Li, and R. Chornock, *Astrophys. J.* **730**, 119 (2011) **732**, 129(E) (2011).
- [47] N. Suzuki *et al.*, *Astrophys. J.* **746**, 85 (2012).
- [48] H. Kodama and M. Sasaki, *Prog. Theor. Phys. Suppl.* **78**, 1 (1984).
- [49] C. P. Ma and E. Bertschinger, *Astrophys. J.* **455**, 7 (1995).
- [50] L. Pogosian and A. Silvestri, *Phys. Rev. D* **77**, 023503 (2008).
- [51] N. A. Lima, *Phys. Rev. D* **89**, 083527 (2014).
- [52] A. A. Starobinsky, *JETP Lett.* **86**, 157 (2007).
- [53] N. A. Lima, V. S. -Barreto, and L. Lombriser, *Phys. Rev. D* **94**, 083507 (2016).
- [54] S. Boughn and R. Crittenden, *Nature (London)* **427**, 45 (2004).
- [55] P. A. R. Ade *et al.* (Planck Collaboration), *Astron. Astrophys.* **594**, A21 (2016).
- [56] G. Cabass, M. Gerbino, E. Giusarma, A. Melchiorri, L. Pagano, and L. Salvati, *Phys. Rev. D* **92**, 063534 (2015).
- [57] L. Lombriser and A. Taylor, *J. Cosmol. Astropart. Phys.* **11** (2015) 040.
- [58] B. Boisseau, G. Esposito-Farèse, D. Polarski, and A. A. Starobinsky, *Phys. Rev. Lett.* **85**, 2236 (2000).
- [59] S. Tsujikawa, *Phys. Rev. D* **76**, 023514 (2007).
- [60] A. D. Felice, T. Kobayashi, and S. Tsujikawa, *Phys. Lett. B* **706**, 123 (2011).
- [61] R. Caldwell, A. Cooray, and A. Melchiorri, *Phys. Rev. D* **76**, 023507 (2007).
- [62] L. Amendola, M. Kunz, and D. Sapone, *J. Cosmol. Astropart. Phys.* **04** (2008) 013.
- [63] S. More, H. Miyatake, R. Mandelbaum, M. Takada, D. Spergel, J. Brownstein, and D. P. Schneider, *Astrophys. J.* **806**, 2 (2015).
- [64] P. A. R. Ade *et al.* (Planck Collaboration), *Astron. Astrophys.* **594**, A24 (2016).
- [65] F. Beutler, C. Blake, M. Colless, D. H. Jones, L. Staveley-Smith, G. B. Poole, L. Campbell, Q. Parker, W. Saunders, and F. Watson, *Mon. Not. R. Astron. Soc.* **423**, 3430 (2012).
- [66] L. Samushia, W. J. Percival, and A. Raccanelli, *Mon. Not. R. Astron. Soc.* **420**, 2102 (2012).
- [67] R. Tojeiro, W. Percival, J. Brinkmann, J. Brownstein, D. Eisenstein, M. Manera, C. Maraston, C. McBride, D. Muna, B. Reid *et al.*, *Mon. Not. R. Astron. Soc.* **424**, 2339 (2012).
- [68] S. Alam *et al.* (BOSS), *Mon. Not. R. Astron. Soc.* **470**, 2617 (2017).

- [69] C. Blake *et al.*, *Mon. Not. R. Astron. Soc.* **425**, 405 (2012).
- [70] S. de la Torre, L. Guzzo, J. A. Peacock, E. Branchini, A. Iovino, B. R. Granett, U. Abbas, C. Adami, S. Arnouts, J. Bel *et al.*, *Astron. Astrophys.* **557**, A54 (2013).
- [71] W. J. Percival *et al.*, *Mon. Not. R. Astron. Soc.* **353**, 1201 (2004).
- [72] Y.-S. Song and W. J. Percival, *J. Cosmol. Astropart. Phys.* **10** (2009) 004.
- [73] C.-H. Chuang and Y. Wang, *Mon. Not. R. Astron. Soc.* **435**, 255 (2013).
- [74] C.-H. Chuang *et al.*, *Mon. Not. R. Astron. Soc.* **461**, 3781 (2016).
- [75] L. Samushia *et al.*, *Mon. Not. R. Astron. Soc.* **439**, 3504 (2014).
- [76] H. Nersisyan, A. F. Cid, and L. Amendola, *J. Cosmol. Astropart. Phys.* **04** (2017) 046.